7.1 SELECTION OF PHYTOPHARMACEUTICALS PRONE TO BE ADULTERATED

Herbal medicines having proven health benefits as per scientific and clinical studies are referred to as phytopharmaceuticals. As per USFDA, adulterated herbal drugs are those which are impure, unsafe, or unwholesome. When it comes to herbal drugs, adulteration generally occurs in lifestyle medicines like in protein powders for energy, anorectics, aphrodisiacs etc for quicker pharmacological effect. Recently many cases about adulteration of herbal aphrodisiacs with their chemical counterparts have been reported. Among the formulary of drugs used for aphrodisiacs, Withania somnifera stand outs to be one of the vital constituent. Due to upsurge in recent past not much analytical studies have been done for investigating the adulteration of herbal formulations. Though studies on analytical studies for estimation of generally used chemical aphrodiasiacs like Sildenafil, Verdanafil, Tadalafil in their pharmaceutical formulations are reported. [1, 2, 3-11] Despite of the reports available, no analytical profile for differentiation of counterfiets with authentics and placebos utilizing DOE based HPLC method and statistical models like HCA and PCA based on chemometrics techniques for NIR, FTIR and Raman spectroscopy data were available in literature for checking their counterfeiting in authentic Ashwagandha herbal tablets.

7.2 DRUG PROFILES OF SYNTHETIC ANALOGUES BEING COUNTERFEITED [12]

Chemical name: Sildenafil

IUPAC Name: 1-((3-(6, 7-dihydro-1-methyl-7-oxo-3-propyl-1H-pyrazolo(4,3-d)pyrimidin-5-yl)-4-ethoxyphenyl)sulfonyl)-4-methylpiperazine citrate

Molecular Formula: $C_{22}H_{30}N_6O_4S$

Molecular Weight: 474.58 gm/mol

Chemical Structure:

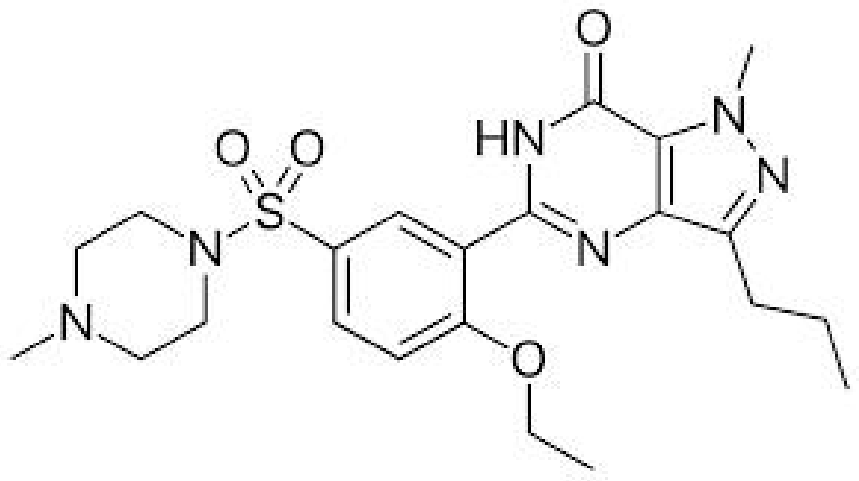

Figure 7.1: Structure of Sildenafil

Appearance: White to off-white crystalline powder

Log P: 1.90

Melting point: 189- 190 °C

pKa: 5.99

Solubility: Freely soluble in water.

Drug Category: Phosphodiesterase (PDE) inhibitors.

Mechanism of action: Sildenafil treats erectile dysfunction by increasing blood flow to the penis during sexual stimulation. This increased blood flow can cause an erection. Sildenafil treats PAH by relaxing the blood vessels in the lungs to allow blood to flow easily.

Uses: Aphrodiasiac, pulmonary arterial hypertension (PAH)

Marketed Formulation:
Viagra tablets having 25, 50, 100 mg of Sildenafil (Pfizer)
Actavis tablets having 25, 50, 100 mg of Sildenafil (Actavis)
Sildenafil film coated tablet having 100 mg of Sildenafil (Torrent Pharma)
Cenforce 100 tablets having 100 mg of Sildenafil (Centurian laboratories)

Chemical name: Tadalafil

IUPAC Name: (2R, 8R)-2-(1,3-benzodioxol-5-yl)-6-methyl-3,6,17-triazatetracyclo heptadeca-1(10),11,13,15-tetraene-4,7-dione

Molecular Formula: $C_{22}H_{19}N_3O_4$

Molecular Weight: 389.41 gm/mol

Chemical Structure:

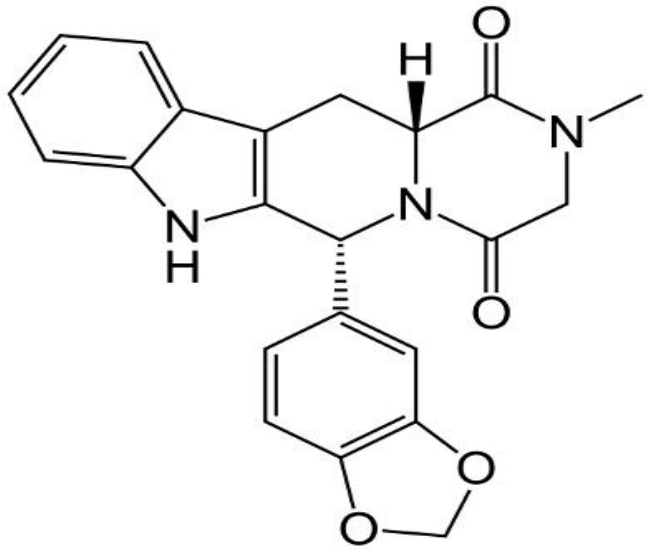

Figure 7.2: Structure of Tadalafil

Appearance: White to off-white crystalline powder

Log P: 1.70

Melting point: 301-302 °C

pKa: 15.17

Solubility: Freely soluble in water and acetonitrile.

Drug Category: Phosphodiesterase (PDE) inhibitors.

Mechanism of action: Tadalafil treats erectile dysfunction by increasing blood flow to the penis during sexual stimulation. This increased blood flow can cause an erection. Tadalafil treats PAH by relaxing the blood vessels in the lungs to allow blood to flow easily.

Uses: Aphrodiasiac, pulmonary arterial hypertension (PAH)

Marketed Formulation:
Cialis tablets having 2.5, 5, 10, 20 mg of Tadalafil (Eli lily)
Tadalafil film coated tablet having 20 mg of Tadalafil (Mylan)
Tadalafil film coated tablet having 20 mg of Tadalafil (Actavis)
Tadalafil film coated tablet having 20 mg of Tadalafil (Sandoz)

Chemical name: Verdenafil

IUPAC Name: 2-[2-ethoxy-5-(4-ethylpiperazin-1-yl) sulfonyl phenyl]-5-methyl-7-propyl-3H-imidazo [5,1-f][1,2,4]triazin-4-one

Molecular Formula: $C_{23}H_{32}N_6O_4S$

Molecular Weight: 488.61 gm/mol

Chemical Structure:

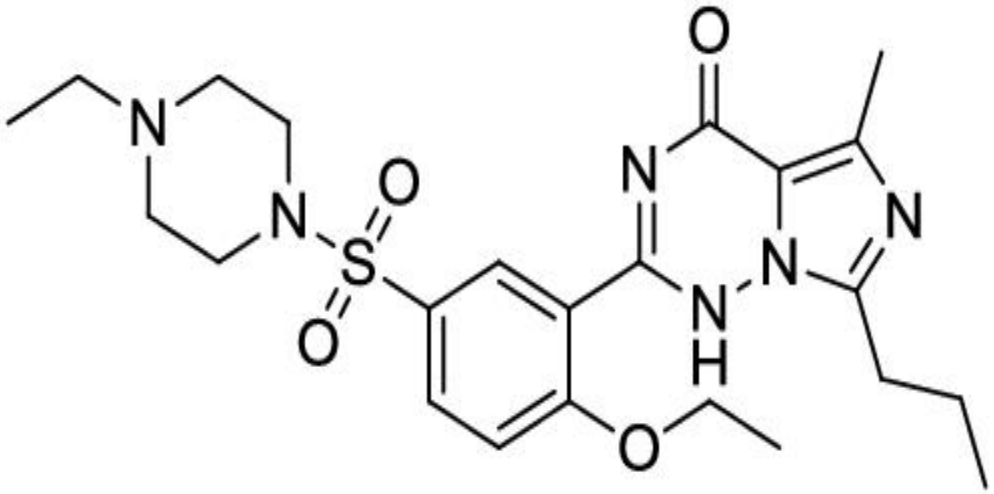

Figure 7.3: Structure of Verdenafil

Appearance: White to off-white crystalline powder

Log P: 1.40

Melting point: 191- 192 °C

pKa: 4.72, 6.21

Solubility: Freely soluble in water

Drug Category: Phosphodiesterase (PDE) inhibitors.

Mechanism of action: Verdenafil treats erectile dysfunction by increasing blood flow to the penis during sexual stimulation. This increased blood flow can cause an erection. Verdenafil treats PAH by relaxing the blood vessels in the lungs to allow blood to flow easily.

Uses: Aphrodiasiac, pulmonary arterial hypertension (PAH)

Marketed Formulation:
Levitra tablets having 2.5, 5, 10, 20 mg of Verdenafil (Bayer)
Vilitra tablets having 20 mg of Verdenafil (Centurian laboratories)
Verdenafil film coated tablet having 20 mg of Verdenafil (Accord)
Valif 20 tablets having 20 mg of Verdenafil (Ajanta)

7.3 DRUG PROFILE OF ASHWAGANDHA AND POTENT CHEMICAL CONSTITUENTS IN WITHANOLIDES TAKEN AS HERBAL MARKER

Chemical name: Ashwagandha [13]

Binomial name: Withania Somnifera

Common name: Indian Winter cherry or Indian Ginseng

Family: Solanaceae

Chemical constituents: The active constituents on Ashwagandha comprises of alkaloids, steroidal lactones and saponins. Alkaloids present in ashwagandha like isopelletierine, cuseohygrine, anaferine etc are having anti-stress acticvity. The main immuno-modulatory activity of Ashwagandha is due to steroidal lactones like withanolides and withaferins.

Uses: The root of Ashwagandha is regarded as tonic, aphrodisiac, narcotic, diuretic, anthelmintic, astringent, thermogenic and stimulant.

Also the leaves, flowers, seeds are used for pharmacological activity. They are having various uses like adaptogenic, aphrodiasiac, diuretic,

Chemical name: Withanolide A

IUPAC Name: (1S,2S,4S,5R,10R,11S,14S,15S,18S)-15-[(1R)-1-[(2R)-4,5-dimethyl-6-oxo-2,3-dihydropyran-2-yl]-1-hydroxyethyl]-5-hydroxy-10,14-dimethyl-3 oxapentacyclooctadec-7-en-9-one

Molecular Formula: $C_{28}H_{38}O_6$

Molecular Weight: 470.61 gm/mol

Chemical Structure:

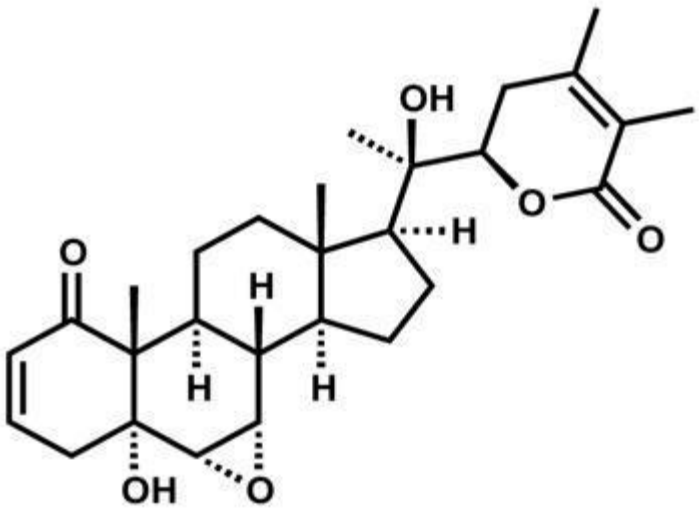

Figure 7.4: Structure of Withanolide A

Appearance: White powder

Log P: 3.3

Melting point: 305 °C

pKa: 13.02

Solubility: Freely soluble in methanol, water.

Drug Category: Steroids

Biological activity: The unsaturation at α, β position of ketone ring in ring A and epoxy group at position 5β, 6β in ring B are necessary for biologically activity of Withanolides.

Uses: Anti-inflammatory, antitumor, antioxidant, antiulcers, bacterial infections and aphrodiasiac

Chemical name: Withaferin A

IUPAC Name: (1*S*,2*R*,6*S*,7*R*,9*R*,11*S*,12*S*,15*R*,16*S*)-6-hydroxy-15-[(1*S*)-1-[(2*R*)-5-(hydroxymethyl)-4-methyl-6-oxo-2,3-dihydropyran-2-yl]ethyl]-2,16-dimethyl-8 oxapenta cyclo octadec-4-en-3-one

Molecular Formula: $C_{28}H_{38}O_6$

Molecular Weight: 470.61 gm/mol

Chemical Structure:

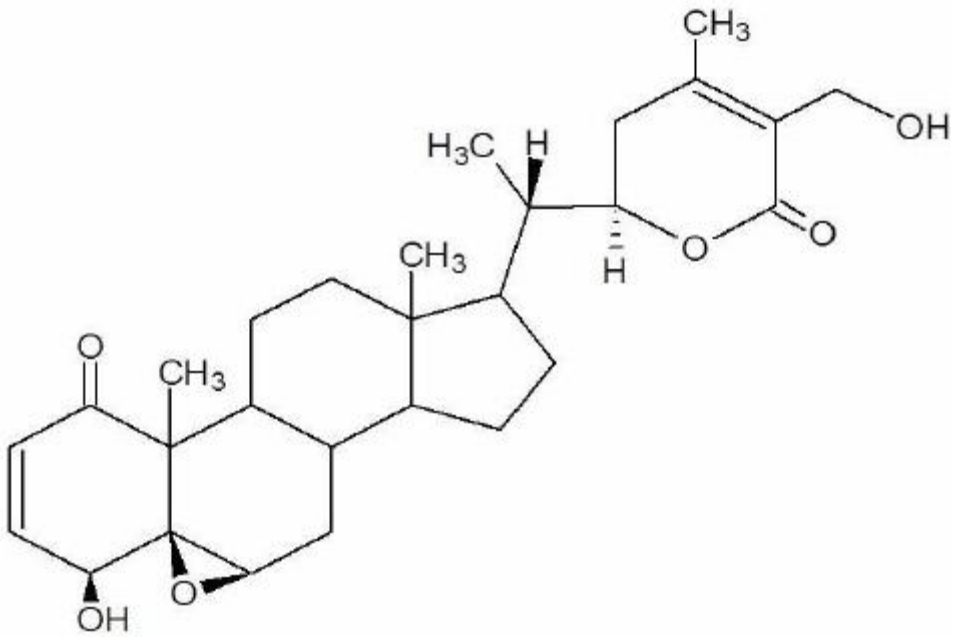

Figure 7.5: Structure of Withaferin A

Appearance: White powder

Log P: 3.80

Melting point: 252-253 °C

Solubility: Soluble in DMSO (20 mg/ml), methanol (10 mg/ml) or 100% ethanol and water.

Drug Category: Steroids

Biological activity: The unsaturation at α, β position of ketone ring in ring A and epoxy group at position 5β, 6β in ring B are necessary for biologically activity of Withanolides.

Uses: Anti-inflammatory, antitumor, antioxidant, antiulcers, bacterial infections and aphrodiasiac

7.4 LITERATURE REVIEW

Various methods have been reported for estimation of synthetic phosphodiesterase inhibitors like Sildenafil, Verdenafil and Tadalafil in pharmaceutical preparations using techniques like HPLC [1], GC-MS [23] etc. For checking the adulteration of Sildenafil, verdenafil and tadalafil in dietary supplements, LC-MS [19] as well as LC-MS-MS [1,11] were reported. Specially for checking their adulteration in Yemen as well as Malaysian market, HPLC methods were reported. [5,10] For individual analysis of these phosphodiesterase inhibitors also various methods are available in literature. For analysis of Sildenafil in pharmaceutical dosage form, HPLC methods have been reported. [6] Similarly for analysis of Verdenafil [14] and Tadalafil [15] in pharmaceutical dosage form also HPLC method is reported. Methods for analysis of these phosphodiestereses along with their synthetic analogues have also been reported as their analogues were also found to be adulterated in some of the dietary supplements. [7-9] Chemometrics in combination with other techniques like HPLC, IR, and UV have been widely used for authentication of herbal medicines. [16] XRF technique along with chemometrics has been used for checking adulteration of sildenafil and tadalafil in pharmaceutical formulations. [17] ATR-FTIR technique for characterization of sildenafil and tadalafil tablets was developed specially for Brazilian market. [18] Also a Raman spectroscopy technique was developed for screening sildenafil. [19] A NIR technique was also reported for checking counterfeiting of Sildenafil, verdenafil and tadalafil. [20] Also quantitative analysis of Withanolides in Ashwagandha formulations by chromatographic methods has been reported. [21-23]

7.5 SECTION –A

7.5.1 Experimental

Development and validation of simple RP-HPLC method for checking adulteration of Sildenafil citrate, Verdenafil, Tadalafil in Ashwagandha herbal tablets

Herbal drugs as we know consist of numerous active constituents having various health benefits. The main chemical constituents of Withania somnifera which is the model herbal drug selected for our study consist of alkaloids, steroidal lactones and saponins. [30] Due to these chemical constituents, Ashwagandha exhibits uses like tonic, aphrodisiac, narcotic, diuretic, anthelmintic, astringent, thermogenic and stimulant etc. [24] As per one of the study majority of activity exhibited by Withania somnifera is due to its two chemical constituents Withanferin A and Withanolide A. [25] Thus, to prevent interference in the chromatogram due to the other chemical constituents of Withania somnifera, HPLC method was developed using herbal markers of Withaferin A and Withanolide A for checking the adulteration of Ashwagandha with synthetic phosphodiasterase 5 inhibitors. After method optimization, the method was applied to ashwagandha tablets where it showed interference along with the main peaks in the chromatogram, which may be due to the chemical constituents other than Withanferin A and Withanolide A.

7.5.1.1 Chemicals and materials

Six brands of Ashwagandha herbal tablets namely Lion (LN), Gondal (GD), Himalaya (HM), Asfa (AF), Charan (CN) and GY. Hakim (GH) was procured from local pharmacy. The active pharmaceutical ingredients of sildenafil (SIL) and verdenafil (VER) were kindly supplied as a gift sample by Centurian laboratories Pvt Ltd, Vadodara Gujarat and the active pharmaceutical ingredient of tadalafil (TAD) was kindly supplied as gift sample from Ami lifesciences Pvt. Ltd, Vadodara, India. The active constituents of Withanolide A (WDA) and Withaferin A (WFA) were procured from Xenon Biosciences, Hyderabad. The excipients used for preparation of placebo samples i.e. sodium starch glycolate, microcrystalline cellulose, talc, titanium dioxide, magnesium stearate, starch, cross povidone, lactose were procured from SD Fine Chemicals. HPLC grade acetonitrile and methanol were procured from Fischer Scientific Pvt Ltd. (India). Double distilled water was prepared at laboratory premises. Unless otherwise specified, all solutions were filtered through a 0.2 µm Nylon 6, 6 membrane filter, Ultipor® N66® from Pall Life Sciences, USA; prior to use.

7.5.1.2 Equipments and analysis conditions

UV Spectroscopy analysis for deriving the suitable wavelengths for estimation of drugs were identified by scanning over the range of 200–400 nm with a Shimadzu UV-1700 double beam spectrophotometer (Shimadzu, Japan). The spectroscopic analysis is carried out using UV probe software.

Chromatographic analysis was carried out on a Waters, Ahmedabad (from Waters Acquity Corporation, Milford, MA, USA) and consisting of following components a gradient pump, PDA detector, a manual injection facility with 20 µl fixed loop, low pressure gradient flow control valve, column oven, solvent

delivery module. The chromatographic analysis was performed using Empower 3 software on a Waters C_{18} column (250×4.6 mm, 5 µm particle size). Other equipments used were an ultrasonic bath (Analab Scintific Instruments Pvt Ltd, Vadodara), precision analytical balance (A X 120, by Shimadzu Corporation analytical and measuring Instruments division, Kyoto, Japan), pH Meter (Labindia Instruments Pvt. Ltd, Navi Mumbai. The experimental design development and optimization of method was carried out using Design expert 7.0 software. Related calculations were done by Microsoft Excel 2010.

7.5.1.3 Sample preparation and analysis by HPLC method

For checking the adulteration in ASH samples by chromatographic analysis, total fifteen samples were analyzed, of which six were commercial formulation (FM) samples coded as LN, GD, HM, AF, CN and GH, five laboratory prepared counterfeit (CF) samples coded as CF1, CF2, CF3, CF4, CF5 and four placebo (PL) samples coded as PL1, PL2, PL3, PL4. The formulation summary for PL and CF samples is as presented in Table 7.7. CF samples were weighed as per the quantity given in Table 7.7 and then diluted with DDW with sonication for 10 min. The sample thus obtained was filtered using 0.45 µ membrane filters and then diluted using appropriate aliquots to get 10 µg/ml of each analyte added. For PL samples, the excipients were weighed as per the quantity given in Table 7.7 for compressed tablet. The weighed ingredients were diluted in 50 ml of DDW and filtered using 0.45 µ membrane filters prior to use. [13]

The RP-HPLC method was developed for Withanolide A (WDA) and Withaferin A (WFA), a herbal marker for ASH along with the probable synthetic adulterants which may be added for counterfeiting of them.

For development of liquid chromatographic method, first 1000 µ g/ml stock solutions were prepared of active pharmaceutical ingredients prone to be added as adulterants in Ashwagandha formulations. 10 mg each of SIL, VER, and TAD were weighed accurately and transferred into a 10 ml volumetric flask containing DDW and sonicated for 10 min. DDW was added up to the mark to produce stock solutions containing 1000 µg/ml of SIL, VER, TAD. Similarly 1000 µg/ml stock solutions of WDA and WFA which are herbal markers for Ashwagandha formulations were prepared. Then for preparation of working standard solution, 2.5 ml each of SIL, VER, TAD, WDA and WFA was transferred into a 25 ml volumetric flask containing 2.5 ml DDW. DDW was added up to the mark to produce a stock solution containing 100 µg/ml of SIL, VER, TAD, WDA and WFA respectively. Then appropriate aliquots of SIL, VER, TAD, WDA and WFA working standard solutions were taken in different 6 ml volumetric flasks each and diluted up to the mark with mobile phase to obtain final concentrations of 2 - 12 µg/ml.

7.5.1.4 Preliminary trials and need for application of risk based DOE approach

Preliminary trials were taken for understanding the pattern for chromatographic analysis which showed that Withanolide A (WDA) and Withaferin A (WFA)

were satisfactorily separated from the peaks of SIL, VER and TAD. Also TAD showed a significant resolved and symmetric peak from the other two active ingredients, whereas optimization for stable retention time of SIL and VER, asymmetry of SIL and VER and also on the resolution between peaks of SIL and VER needed to be worked out. Symmetric and resolved peaks of five components were needed for development of optimized HPLC method for checking the adulteration SIL, VER and TAD in Withania somnifera which would be a cumbersome task if done by OFAT (One factor at a time) analysis, thus it was decided to move forward with risk based DOE approach.

7.5.1.5 Risk based DOE approach for development of optimized HPLC method

The factors incorporated into the DOE design of HPLC method play very vital role for development and optimized and robust method for the study. Thus, screening of significant factors is of primary importance. For our study, risk assessment was done using CNX approach whereas DOE was applied for screening of significant factors using D-optimal screening design. For development of optimized chromatographic method, 2^4 full factorial designs was applied.

7.5.1.5.1 Risk assessment based on CNX approach for optimization of HPLC method

For development of HPLC method, various method parameters needed to be considered based on response component attributes which can have an effect on system suitability of HPLC method. For the above stated, CNX (Controlled noise and experimental) approach was utilized as shown in Table 7.1 for risk assessment of chromatographic method, which is based on Ishikawa (or cause and effect) diagram. (Figure 7.6)

Figure 7.6 Ishikawa or cause and effect diagram

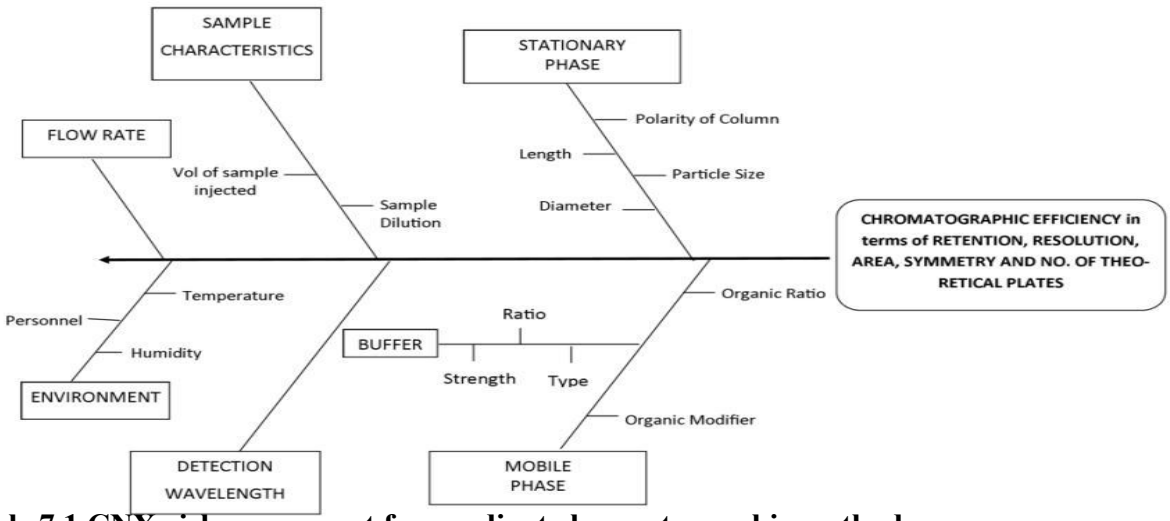

Table 7.1 CNX risk assessment for gradient chromatographic method

Method parameter	Cause	Component attributes			Total score (RPN)	C,N, X	Strategy
	Attibute Score	Resolution	Retention time	Asymmetry of peak			
Column	Stationary phase	10	10	10	300	C	C-18
	Column age	10	10	10	300	N	New column
	Equilibration	5	5	5	150	C	Fixed 30min
Mobile phase	% organic	10	10	10	300	X	DOE
	pH	10	10	10	300	X	DOE
	% of organic modifier (TEA)	10	10	10	300	X	DOE
Pump	Flow rate	5	10	5	200	X	DOE
Heater	Column temperature	1	5	1	70	C	Ambient
Instrumental	Wavelength	5	5	5	150	C	DOE
Instrumental	Hold time	10	10	10	300	N	DOE

Notes: C = controlled, N = Noise, X = Experimental; Scoring: 1 – negligible risk, 5 – low risk (potential impact), 10 – high risk (proven impact) Final score is the summation of each component attribute times the parameter score (10x10+10x10+10x10=300), RPN: Risk priority number

Based on studies of risk assessment from CNX approach, Risk priority number was obtained for each factor as apparent in Table 7.1. For RPN score, 0-100 can be interpreted as minor risk, 101-200 can be interpreted as moderate risk and 201-300 can be interpreted as major risk to be rectified. Based on the RPN score and associated risks for various factors, optimization utilizing DOE needed to be done for mobile phase conditions, instrument conditions and for sample preparation.

7.5.1.5.2 Application of DOE for screening of significant factors for development of optimized method

Then considering the factors which could have a significant impact on the HPLC method as per CNX approach, DOE was applied for screening the factors. For screening purpose D-optimal screening design (Table 7.2) was utilized considering six factors namely pH of mobile phase, Hold time 2, % of Organic ratio at end of Hold time 2, % of TEA, Wavelength, and Flow rate whereas the

five responses which were considered included Resolution between the peaks of SIL and VER, Retention time of SIL and VER, Asymmetry of SIL and VER.

Table 7.2 Variables and their levels for D-optimal design

Factors	Coded values	Actual values
% organic phase at hold time (ml)	-1	75
	+1	80
Hold time in the gradient elution method (min)	-1	6
	+1	7
%TEA in aqueous phase	-1	0.1
	+1	0.2
pH of aqueous solvent in the mobile phase	-1	6
	+1	6.5
Wavelength (nm)	-1	250
	+1	254
Flow rate (ml)/min	-1	0.9
	+1	1
Responses		**Constraints**
R1-Resolution		2≤R1≥4
R2- Asymmetry of SIL and VER		0.5≤R2≥2.0
R3- Asymmetry of VER		0.5≤R3≥2.0
R4 – Retention time of SIL		6≤R4≥7.5
R5 – Retention time of VER		6.5≤R5≥8

Based on statistics like factorial fit values for the five responses (Table 7.3) by the software utilizing the Shapiro-Wilk test and the effects plots namely Pareto chart (Figure. 7.7, 7.8, 7.9, 7.10, 7.11), Residual plots (Figure. 7.12, 7.13, 7.14, 7.15, 7.16) and Main effect plots (Figure. 7.17, 7.18, 7.19, 7.20, 7.21), the factors significantly affecting the method were screened.

Table 7.3 Statistical analysis showing the factorial fit for responses for D-optimal screening design.

Parameters	Resolution	RT of SIL	RT of VER	Asy of SIL	Asy of VER
Std. Dev.	0.256011048	0.272686358	0.569595472	0.136974288	0.209072195
Mean	2.212941176	6.564117647	7.063823529	1.767941176	1.810294118
C.V. %	11.56881399	4.154196685	8.0635575	7.747672264	11.54907334
PRESS	2.909824412	3.116541333	13.08063303	0.919919881	1.95064309
R-Squared	0.769619286	0.534576458	0.192417196	0.919066914	0.765781693

Adj R-Squared	0.7184235771	0.4311490004	0.0129543551	0.9010817784	0.7137331881
Pred R-Squared	0.6211810266	0.2775119978	-0.2059214005	0.8530281244	0.6128829255
Adeq Precision	13.34747065	7.542981394	3.287881835	23.33537033	11.43101487

Figure 7.7 Pareto Chart for response resolution between SIL and VER.

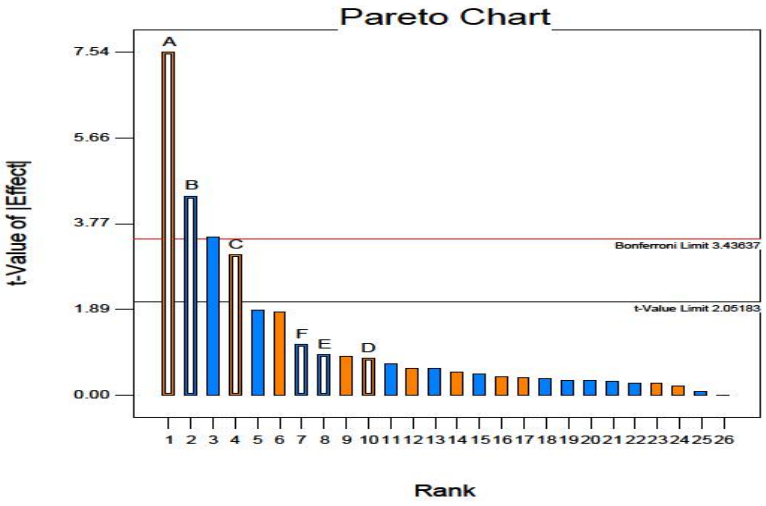

Figure 7.8. Pareto Chart for response retention time of SIL.

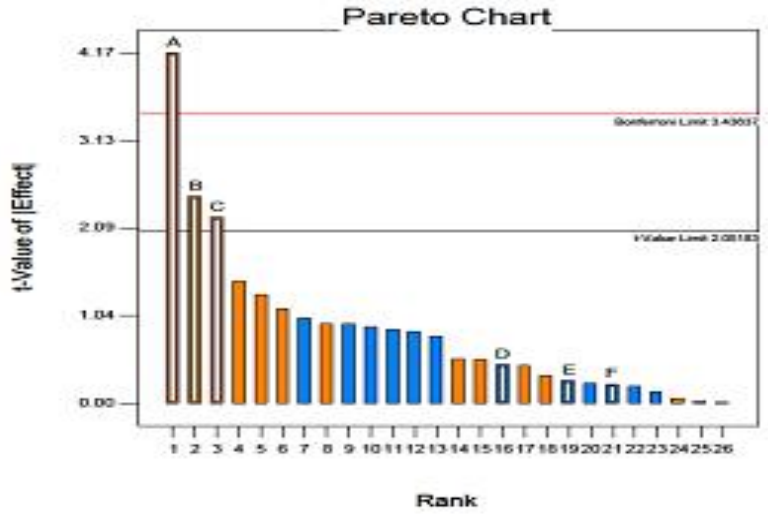

Figure 7.9 Pareto Chart for response retention time of VER.

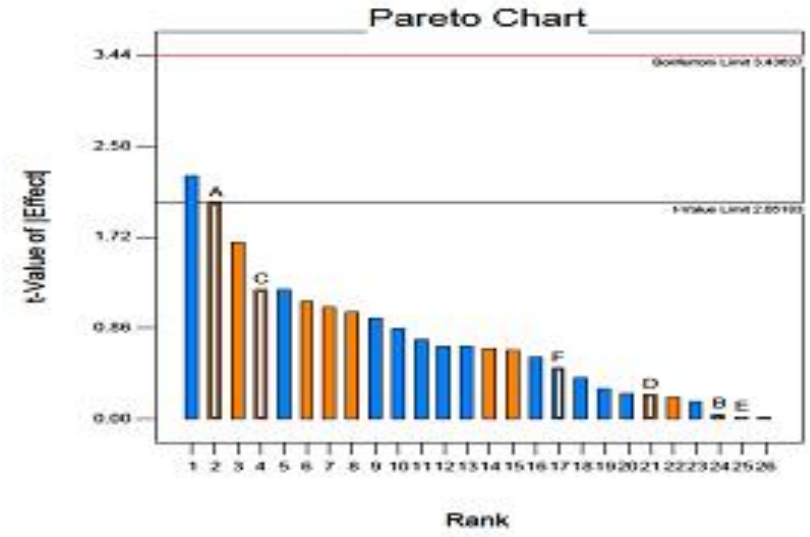

Figure 7.10 Pareto chart for response asymmetry of SIL.

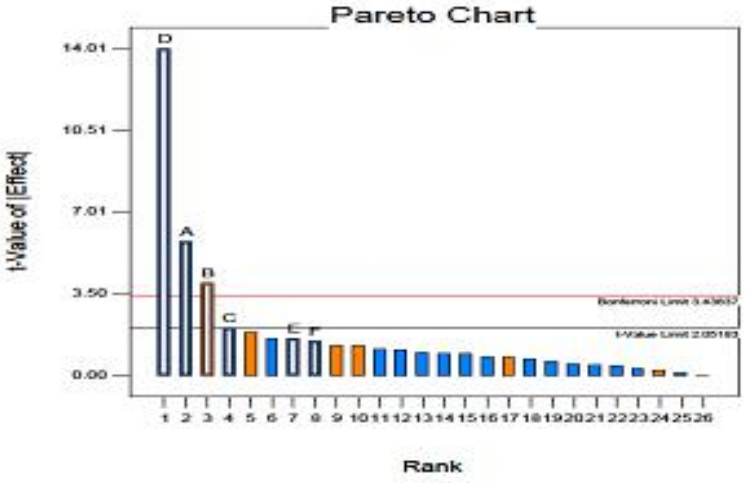

Figure 7.11 Pareto chart for response asymmetry of VER.

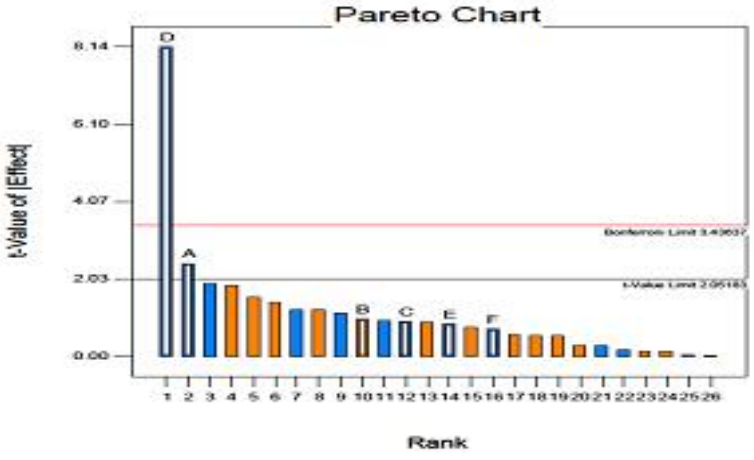

Figure 7.12 Residual plots for response resolution between SIL and VER.

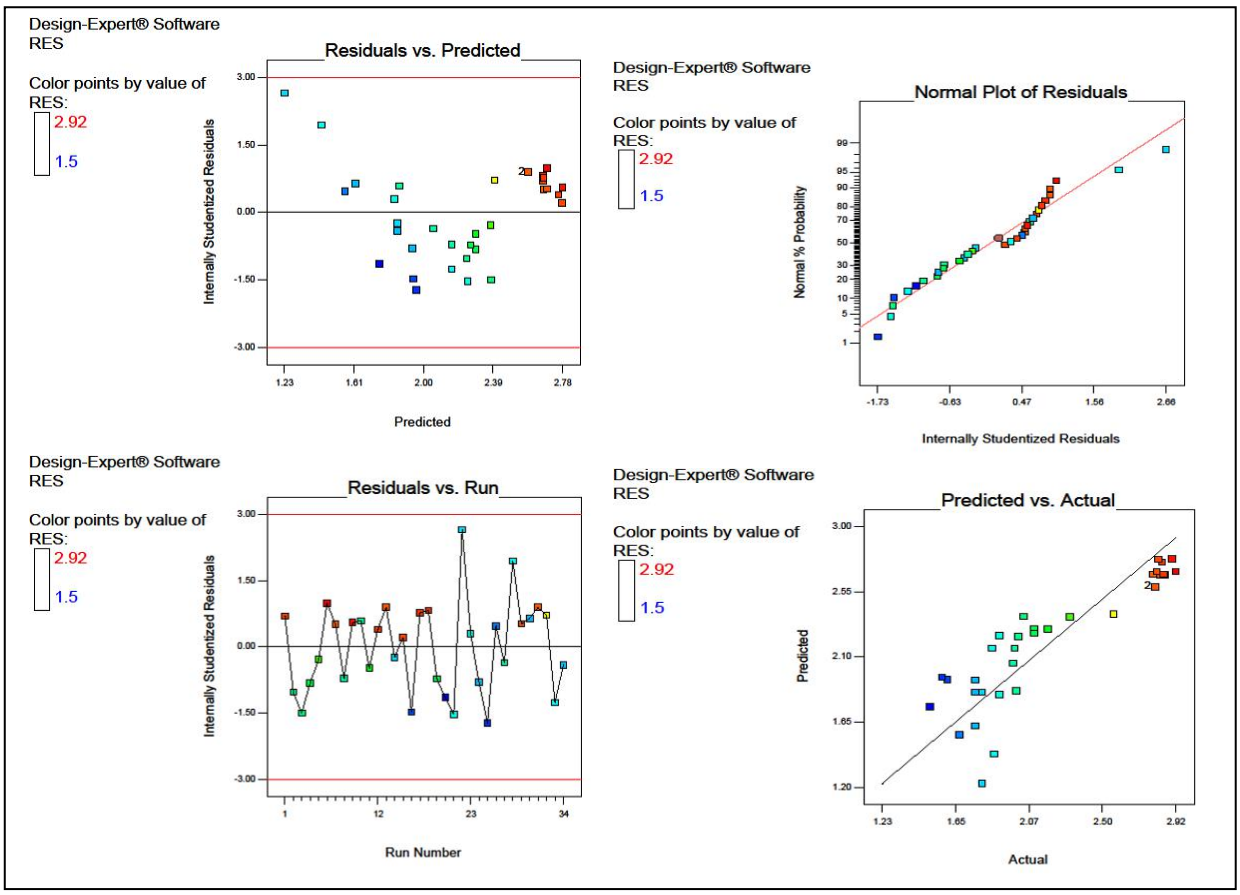

Figure 7.13 Residual plots for response retention time of SIL.

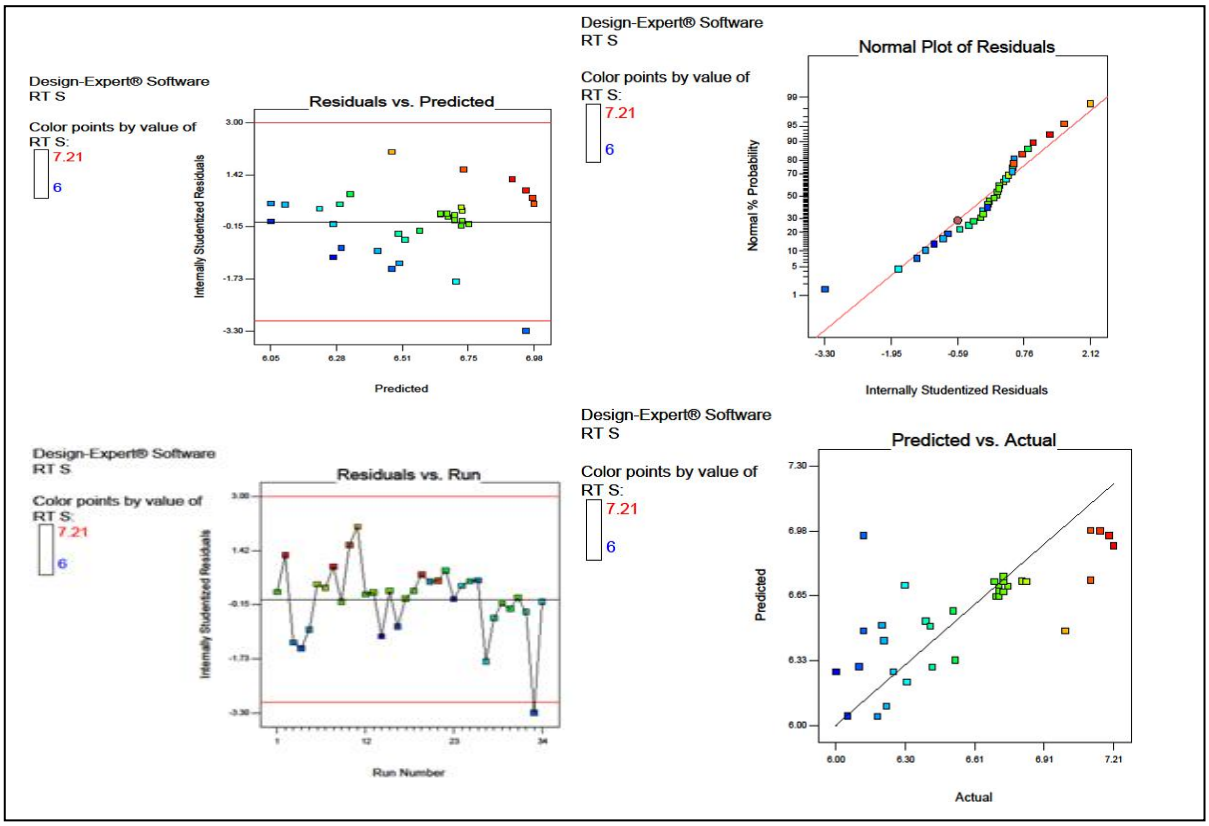

Figure 7.14 Residual plots for response retention time of VER.

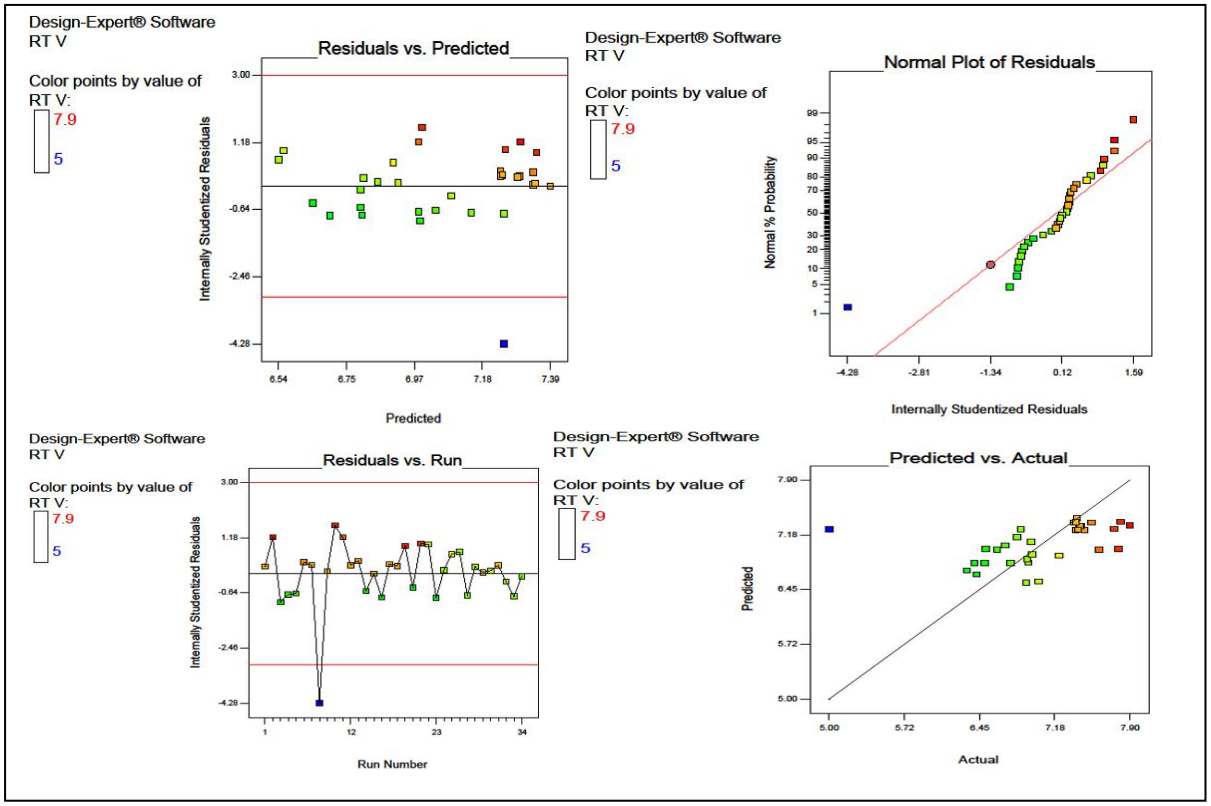

Figure 7.15 Residual plots for response asymmetry of SIL.

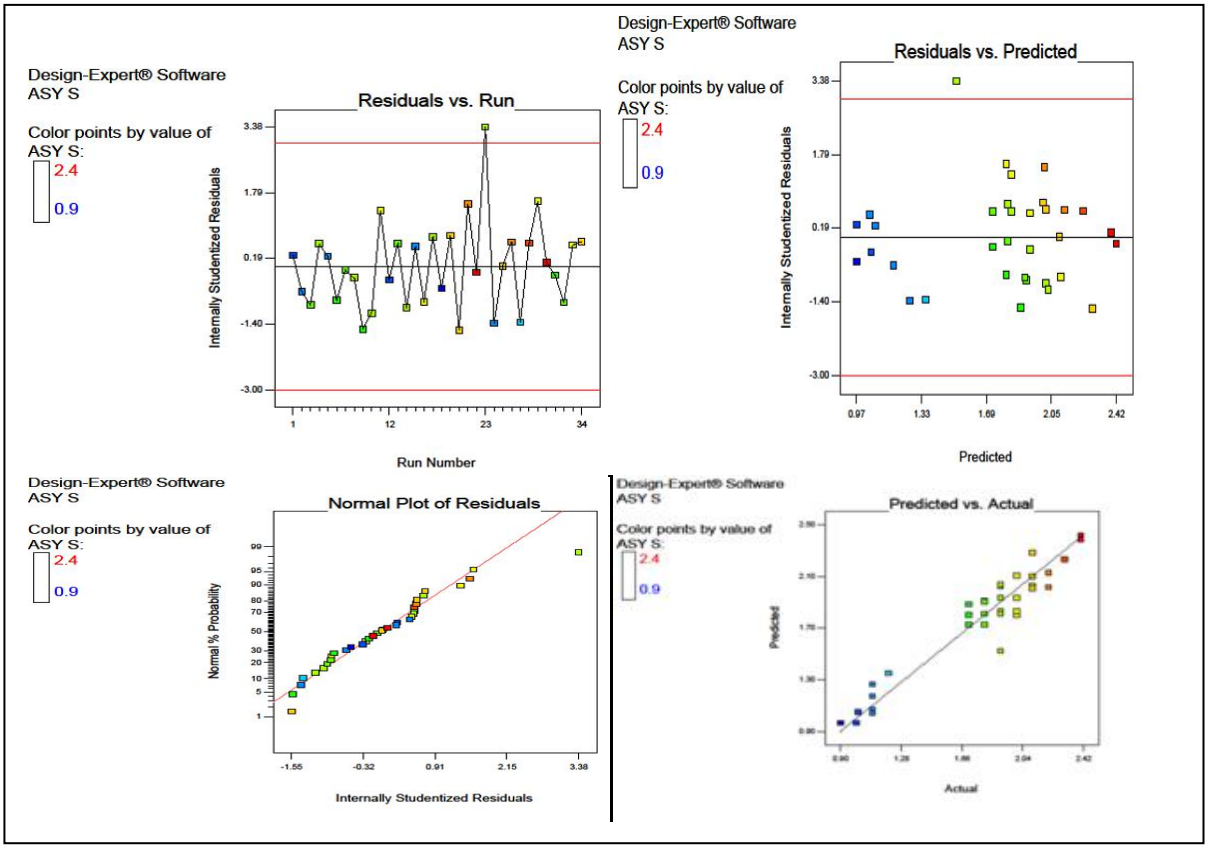

Figure 7.16 Residual plots for response asymmetry of VER.

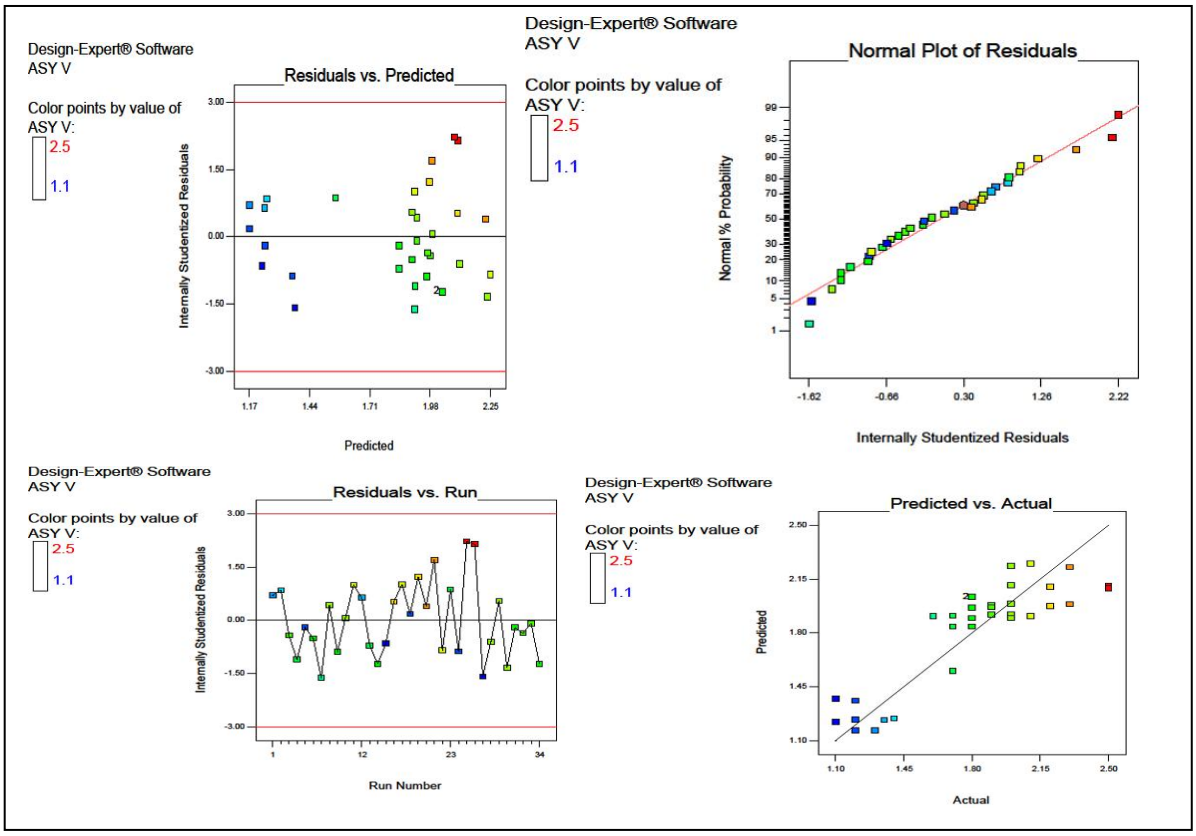

Figure 7.17 Main effects plots of each factor for response Resolution between SIL and VER.

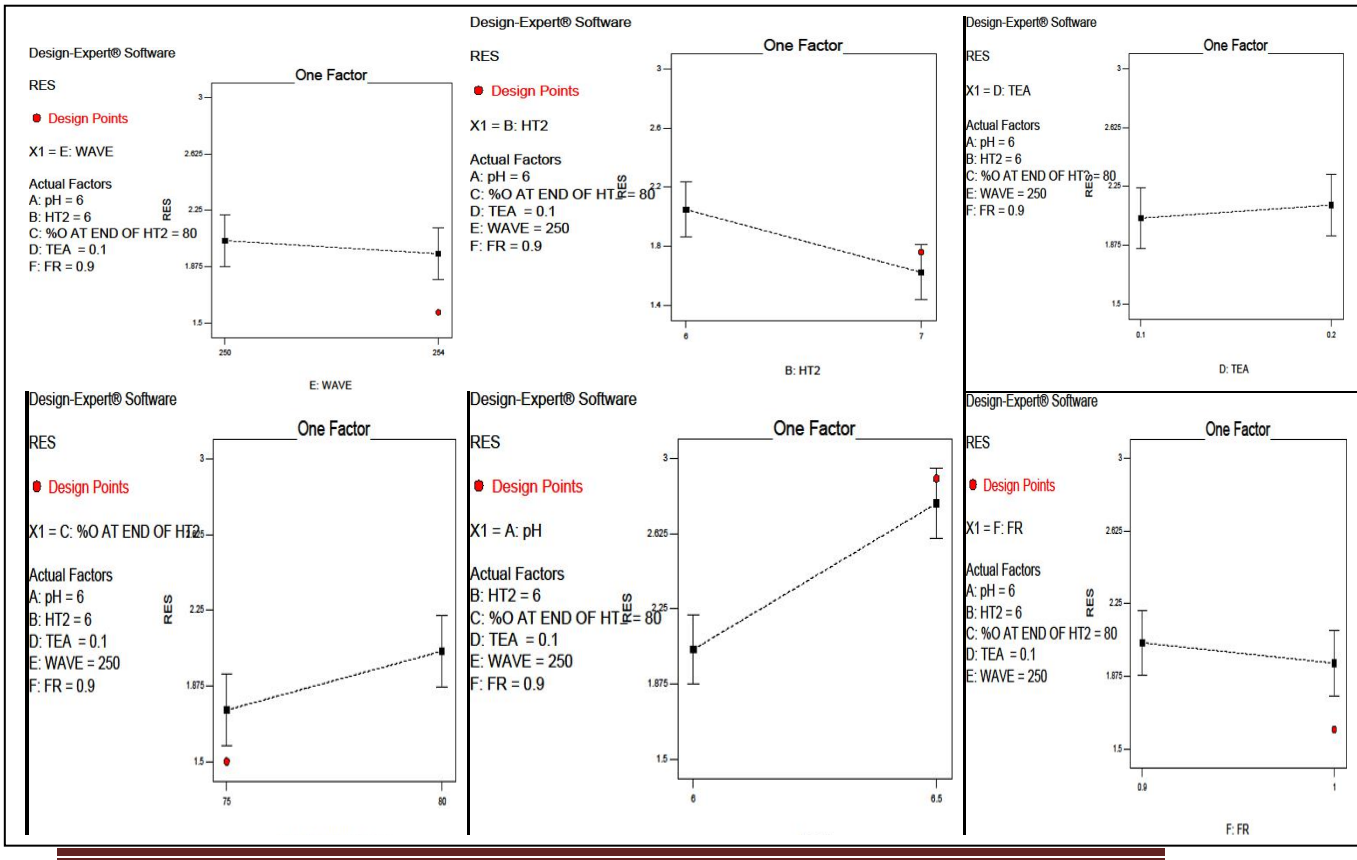

Figure 7.18 Main effects plots of each factor for response retention time of SIL.

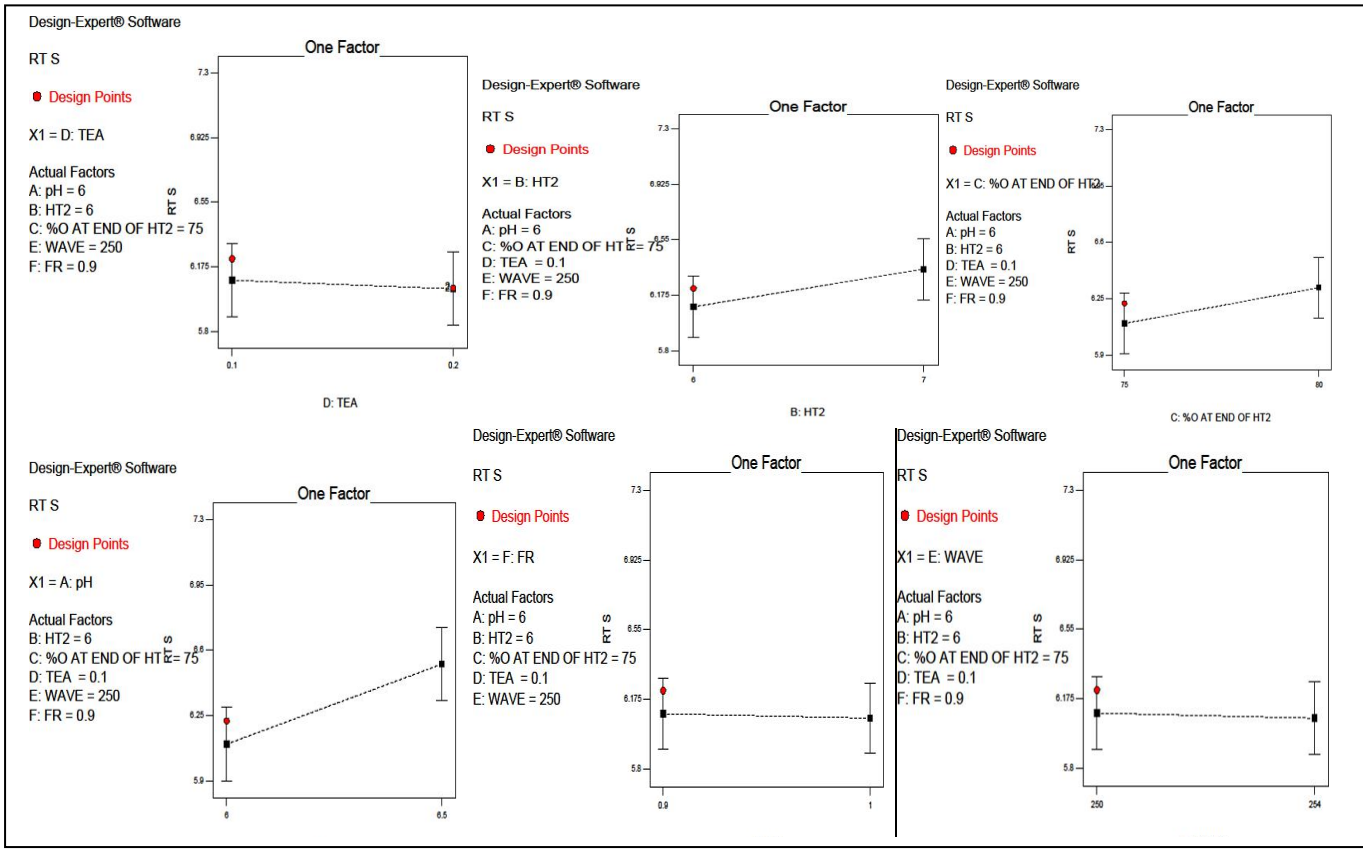

Figure 7.19 Main effects plots of each factor for response retention time of VER.

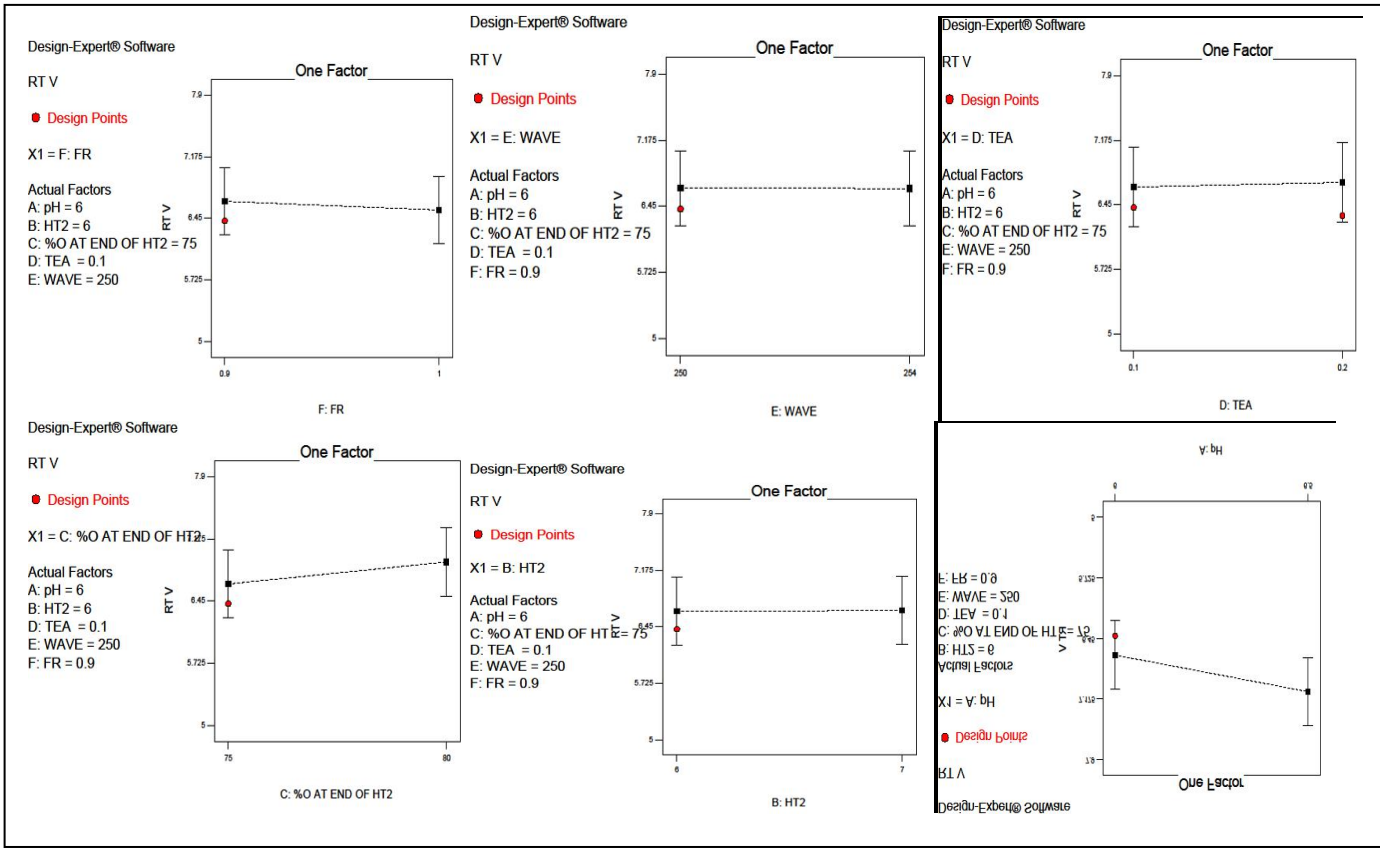

Figure 7.20 Main effects plots of each factor for response asymmetry of SIL

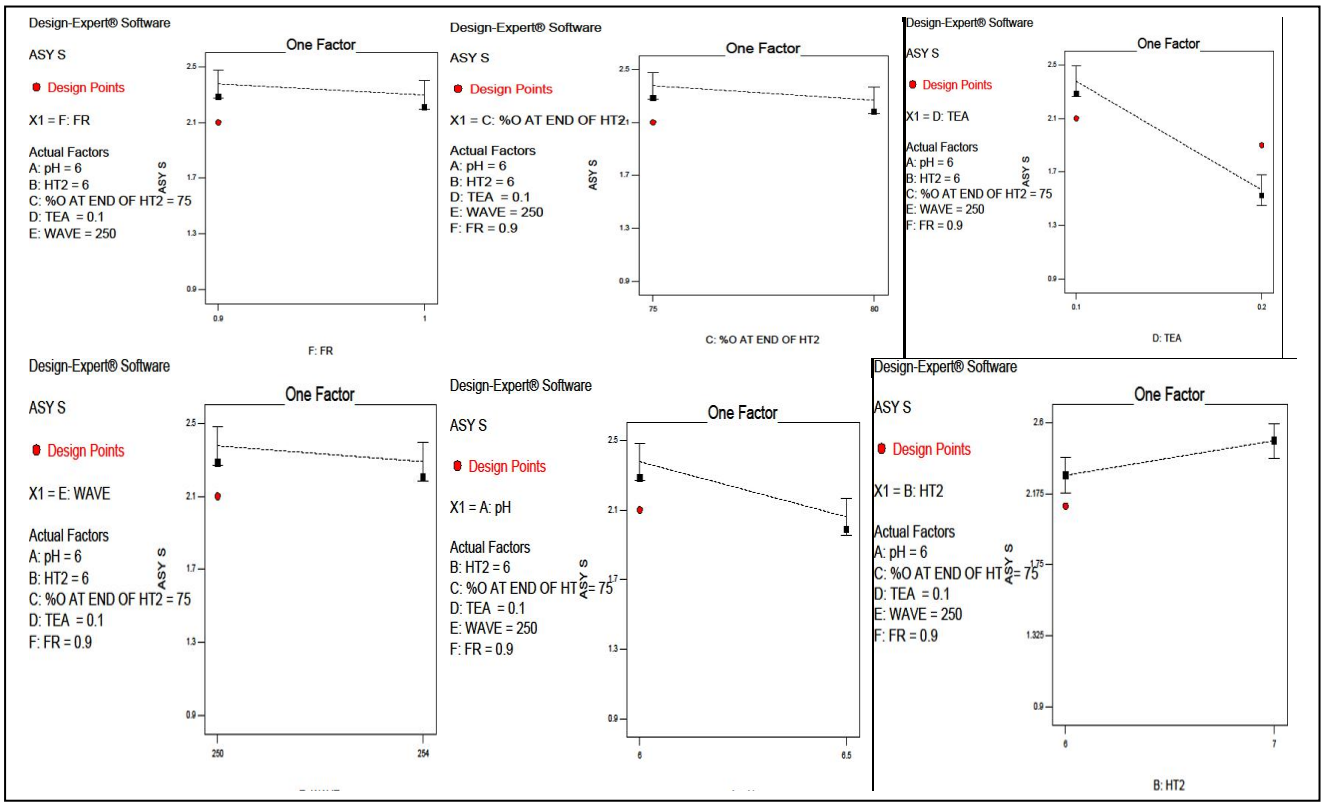

Figure 7.21 Main effects plots of each factor for response asymmetry of VER

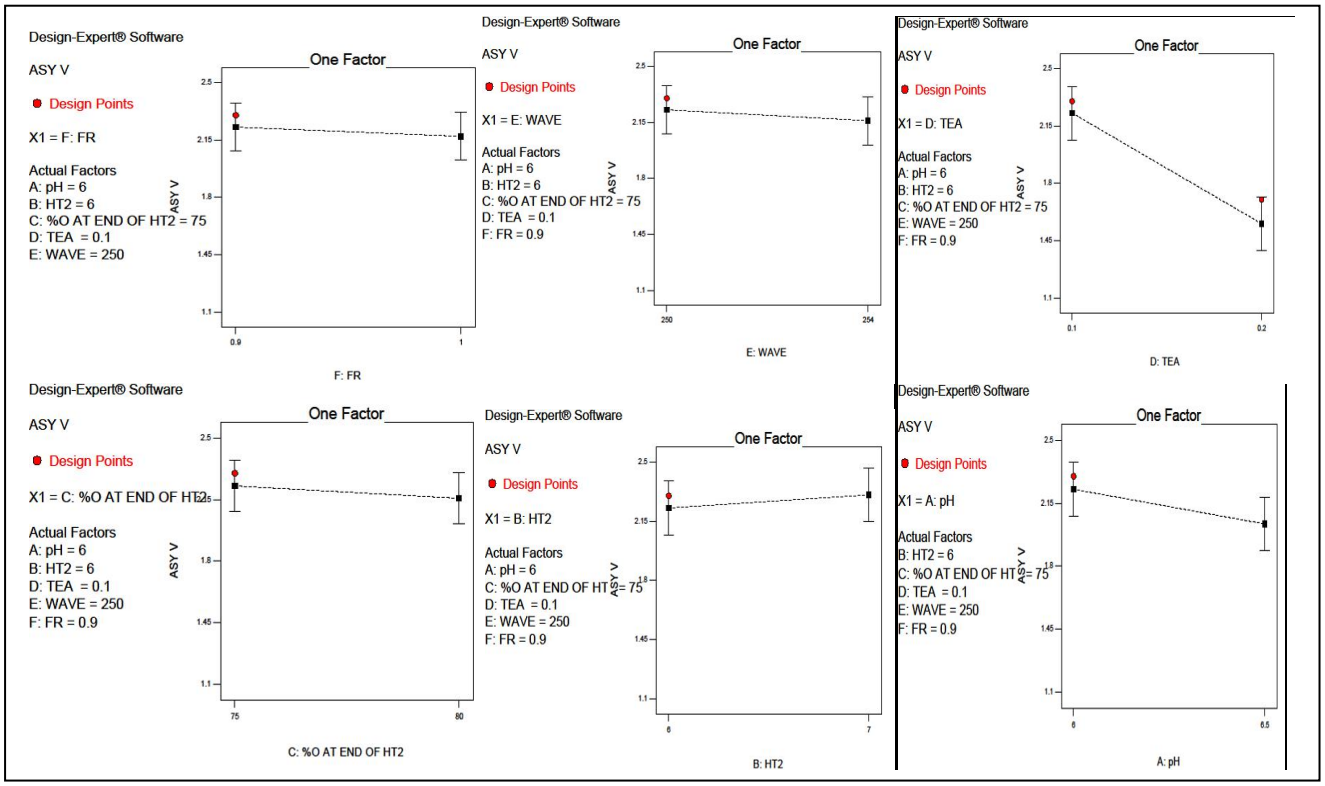

Apparent from the pareto charts, residual and effects plots, the factors having significant impact for optimization of HPLC method screened were % organic phase at hold time (ml), Hold time in the gradient elution method (min)**,** %TEA in aqueous phase and pH of aqueous solvent in the mobile phase.

7.5.1.5.3 2^4 full factorial design for optimization of HPLC method

Then considering the four screened factors, optimization of method was done utilizing 2^4 full factorial design. (Table 7.4) Based on statistics showing factorial fit for responses, mathematical equation for the responses and contour plots for optimization, 17 solutions were obtained. On practical implementation of the solutions, the optimum design space was obtained for chromatographic method.

Table 7.4 Variables and their levels for 2^4 full factorial design

Factors	**Coded values**	**Actual values**
% organic phase at hold time (ml)	-1	70
	0	80
	+1	90
Hold time in the gradient elution method (min)	-1	5
	0	6
	+1	7
%TEA in aqueous phase	-1	0.1
	0	0.2
	+1	0.3
pH of aqueous solvent in the mobile phase	-1	6
	0	6.5
	+1	7
Responses		**Constraints**
R1-Resolution		2≤R1≥4
R2- Asymmetry of SIL and VER		0.5≤R2≥2.0
R3- Asymmetry of VER		0.5≤R3≥2.0
R4 - Retention time of SIL		6≤R4≥7.5
R5 - Retention time of VER		6.5≤R5≥8

7.4.1.6 Method Validation [19]

The method was validated using International Conference on Harmonization (ICH), Q2 (R1) guideline (ICH, 2005) for linearity, range, and precision, limit of detection, limit of quantification, robustness, ruggedness and specificity.

7.5.2 Results and discussion

7.5.2.1 Selection of ATP

For development of optimized chromatographic method, first various preliminary trials were taken. Various mobile phase ratios in isocratic mode were

tried but problem of resolution between peaks of SIL and VER still existed. The peaks of WDA and WFA were well separated from the peaks of active ingredients. Also TAD peak has optimum resolution with respect to other two active ingredients. The optimized method required five resolved peaks, two of withanolides and three of synthetic active ingredients. Thus it was decided to carry out more trials implying DOE and risk based CNX approach.

7.5.2.2 Application of CNX approach for risk assessment and selection of factors affecting the chromatographic method

As previously stated in methodology, six parameters encasing 10 causes were considered for risk assessment as per the CNX approach as shown in Table 7.1. The parameters were selected based on their effect on the chromatographic efficiency in terms of retention, resolution and symmetry which in turn is based on the Ishikawa diagram as represented in Figure. 7.6. In CNX risk assessment every parameter was scored in three gradients viz negligible risk, low risk and high risk contributing score 1, 5 and 10 respectively. From that final score is calculated which is the summation of each component attribute times the parameter score. Based on the summated score which is the risk priority number (RPN), it was decided whether the risk to be controlled, whether it is a major noise or it to be taken care of by experimental design. (Table 7.1) A strategic planning was done based on the RPN score obtained in Table 7.1, which inferred six factors to be undertaken for experimental design, namely % of organic ratio at end of holdtime 2, pH of mobile phase, % of organic modifier (Triethylamine in this case), flowrate, wavelength of detection and hold time 2 for the gradient mobile phase.

7.5.2.3 Application of DOE for screening of factors for optimization of chromatographic method

Now six factors were obtained but the factors actual affecting the method were needed to be screened. DOE was applied in which D-optimal screening design was utilized for screening of significant factors from the six factors obtained after CNX approach, affecting the chromatographic efficiency in terms of five responses namely resolution between SIL and VER, retention time of SIL and VER, asymmetry of SIL and VER. In total 34 trial runs were obtained. The trial runs were practically performed on the HPLC-PDA system and the responses obtained from the runs were entered in the actual design summary generated by the software. Statistical manipulations by the software were done based on the Shapiro-wilk test which gave the factorial fit values for the five responses represented in Table 7.3. From the effects plots (Figure. 7.7 to Figure 7.21), it was inferred that four major factors were significantly affecting the chromatographic efficiency. The four factors were screened based on the Pareto chart, residual plots and main effects plots individually for each of the five responses. Pareto charts explain the degree of effect of each factor on our response in the form of bars. This begins with the most significant response followed by other responses in decreasing order of their contribution to the corresponding factor. For Pareto chart, the factors above the bonferroni limit were considered as significantly affecting factors. From the Pareto charts, it could be concluded that % organic phase in mobile phase is most significant factor for resolution between

SIL and VER, retention time of SIL as well as on retention time of VER, whereas pH of aqueous solvent in mobile phase is having significant effect on the asymmetry of SIL and VER.

For Residual plots, the difference between observed response and fitted response value is said to be its residual. Standardized residuals generally have a variance of 1. Standardized residuals with absolute value >2 are considered very large and treated as unusual observations. Normal Probability of distribution plots the residuals versus the expected values when the distribution is normal. It should roughly follow a straight line. Curved line indicates skewness; nonlinear line indicates non-normality while a point far away indicates outlier. The graph of residual vs. Predicted should be randomly scattered about zero. One of the assumptions of regression and ANOVA is that the variance of error term is constant. In residual vs. Predicted plots; these errors will have a constant variance when the residuals are scattered randomly about zero. Residual vs. Run plots, the data indicates whether there are systematic effects in data due to time or data collection order. Predicted vs. Actual plots shows the effect of the model and compares it against the null model. For a good fit, the points should be close to the fitted line, with narrow confidence bands.

Main effects plots directly mark out the factors which cause significant variation in our critical process parameters. They explain the "absolute" effect of each factor on the given response. Higher deviation from the mean line indicates more significant contribution for the given response.

The factors were screened based on having overall significant effect on almost all responses involved based on the plots described above. Hence, four factors screened for the next stage of optimization of DOE were pH of mobile phase, hold time 2, % of organic ratio at end of hold time 2 and % of organic modifier (% of triethylamine in this case) added in the mobile phase.

7.5.2.4 DOE based HPLC method development using full factorial design

For optimization of method 2^4 full factorial designs was applied considering the four screened factors and five responses as selected for screening design. 21 trial runs were suggested by the software for full factorial design as shown in Table 7.4. The trials were practically implemented and responses entered in the actual design summary generated by the software. Statistical manipulations by the software were done which gave the factorial fit values for the five responses represented in Table 7.5b. For statistics factorial model and 4FI order was selected. From the ANOVA results (Table 7.5 a), which stated p-values for all responses to be less than 0.0500 and equation for ANOVA analysis as well as optimization plots in terms of contour plots for each individual responses stated the model to be significant for optimization of chromatographic method.

7.5.2.4.1 Equations from ANOVA Analysis

Statistical significance can be ascertained by statistical test: ANOVA.

Resolution= 2.67+0.005*A+0.04625*B-0.07625*C+0.00375*D
Retention time of SIL= 6.7375+0*A-0.025*B-0.4875*C+0*D
Retention time of VER=7.16875+0.01875*A-0.00625*B-0.51875*C+0.01875*D
Asymmetry of SIL=1.2+0.025*A-0.0125*B+0.025*C-0.4875*D

Asymmetry of VER=1.1875+0.0125*A-0.05*B+0.0125*C-0.55*D, where
A= pH of mobile phase
B= hold time 2
C= % of organic ratio at end of hold time 2
D=% of organic modifier (% of triethylamine in this case) added in the mobile phase

7.5.2.4.2 Contour plots for different responses

A contour plot is a graphical representation of the relationships among three numeric variables in 2-dimensions. These are geometric illustration of responses obtained by plotting one independent variable vs. another while holding the magnitude of response level and other variables constant. (Figure 7.22 to 7.26)

7.5.2.4.3 Optimization Criteria

For every response, a desired target or range must be specified along with their degree of importance. Based on our input required goals for the responses, software generates various optimized solutions. After analysis, numerical as well graphical optimization was done which gave 17 solutions.

7.5.2.4.4 Point Verification and Working Point selection

Out of the 17 optimized solutions generated by the software, 6 solutions were selected for checkpoint analysis i.e. to verify whether the predicted and experimental results are closely correlated. All these six predictions are tested by experimental trials and the responses observed must lie within 95% confidence interval of their predicted values. One of these solutions was also selected as the final optimized working point for the proposed method as the working point. On implementation of solution, 2D overlay (Figure 7.27) plot as well as 3D overlay plot (Figure 7.28) showing predicted desirability to be 1 in derringer desirability plot (Figure 7.29) optimum design space was obtained for development of chromatographic method. In the design space, yellow region shows the workable region for getting robust analytical results whereas gray region indicates the nonworkable region for optimum robust results. Table 7.5c shows the point verification and working point selection for the proposed working point.

Table 7.5a ANOVA summary 2^4 for full factorial model

Response	Source	Type of Model	Sum of squares	d.f	F-value	P-value Prob.>F-value
Resolution	Model	4FI	0.127875	4	0.163685	< 0.0001
RT of SIL	Model	4FI	3.8125	4	60.10121	< 0.0001
RT of VER	Model	4FI	4.3175	4	42.84651	< 0.0001
Asy of SIL	Model	4FI	3.825	4	76.70455	< 0.0001
Asy of VER	Model	4FI	4.885	4	32.68287	< 0.0001

Table 7.5b Statistical analysis showing the factorial fit for responses using 2^4 full factorial designs for method optimization.

Parameters	Resolution	RT of SIL	RT of VER	Asy of SIL	Asy of VER
Std. Dev.	0.441936	0.125931	0.158719	0.111654	0.193305
Mean	2.707619	6.719524	7.22619	1.166667	1.209524
C.V. %	16.32192	1.874109	2.196438	9.570362	15.98188
PRESS	6.198018	0.496158	0.798918	0.388998	1.181426
R-Squared	0.041824	0.94127	0.919522	0.95339	0.897071
Adj R-Squared	-0.21369	0.925608	0.898061	0.94096	0.869623
Pred R-Squared	-0.96601	0.878157	0.837522	0.904813	0.784336
Adeq Precision	1.224471	15.22736	13.26044	18.43111	12.09767

Figure 7.22 Contour plots for response resolution between peaks of SIL and VER.

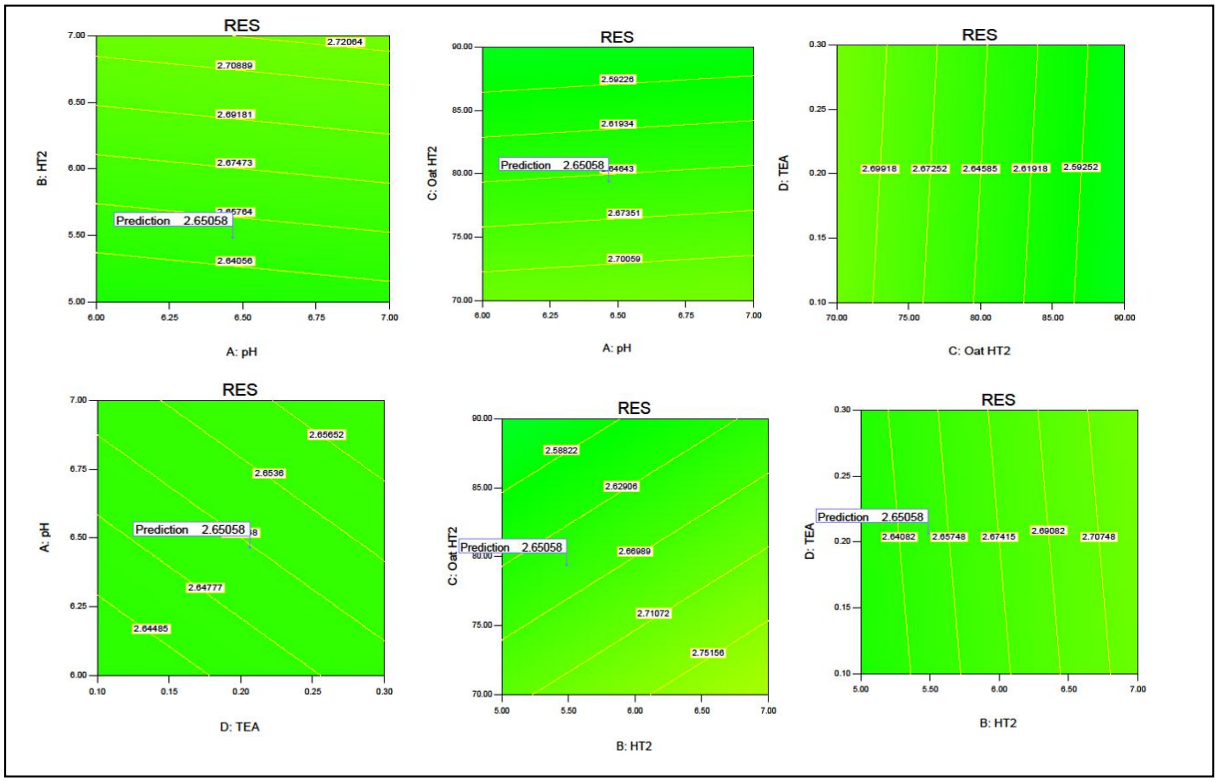

Figure 7.23 Contour plots for response retention time of SIL

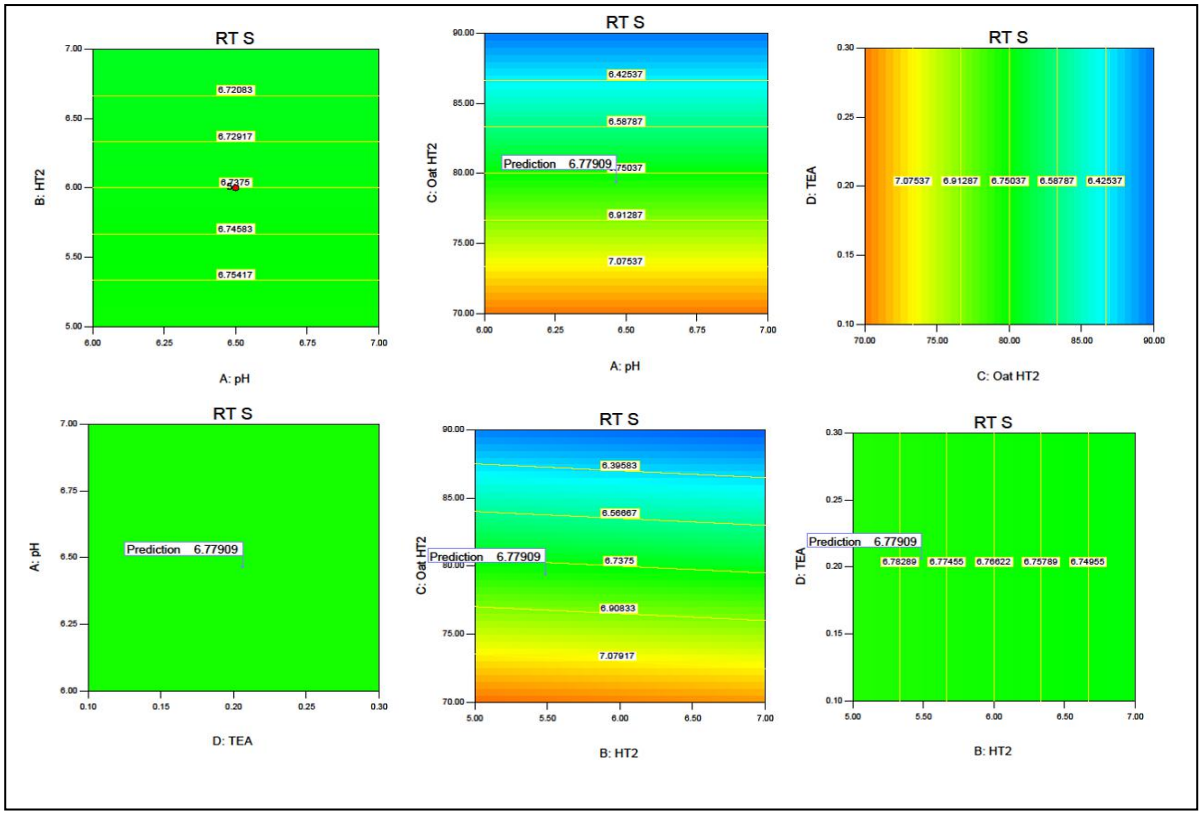

Figure 7.24 Contour plots for response retention time of VER

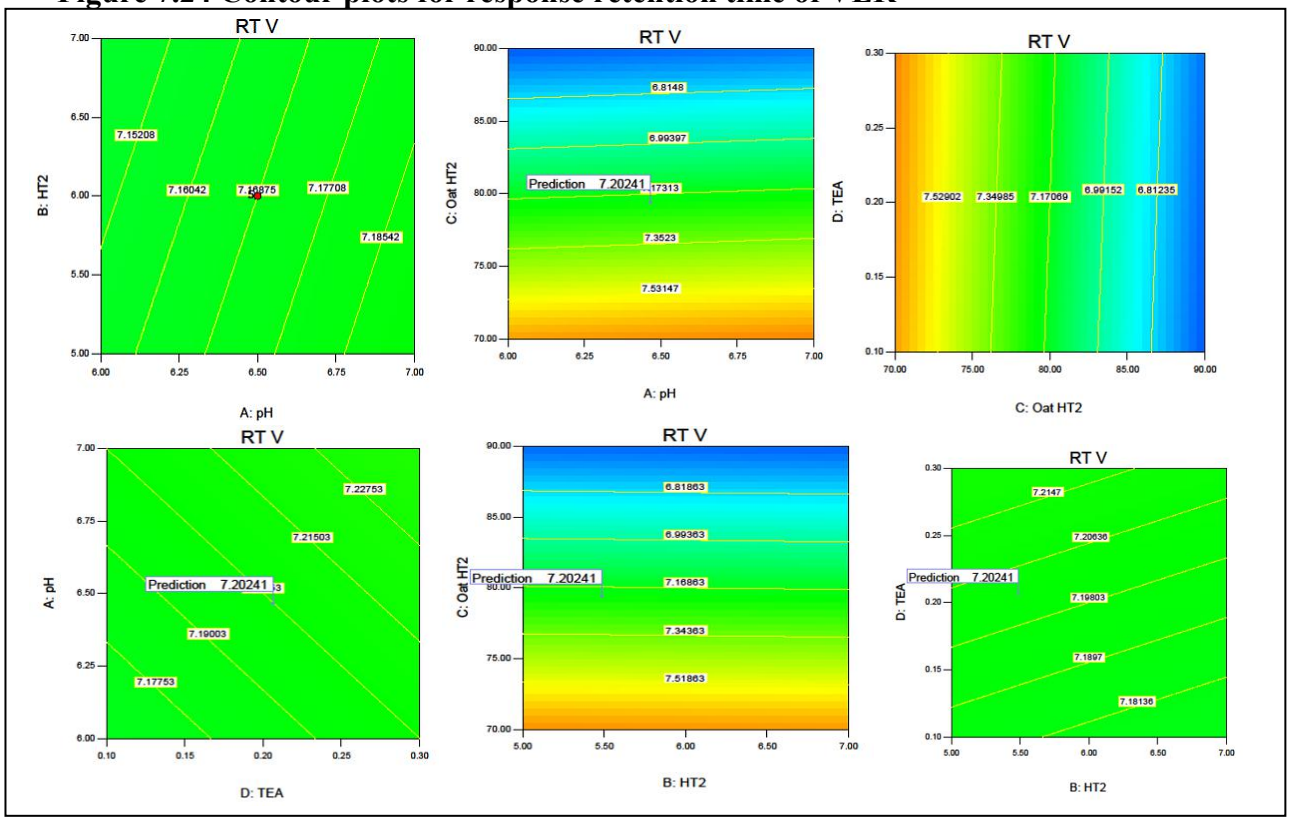

Figure 7.25 Contour plots for response asymmetry of SIL.

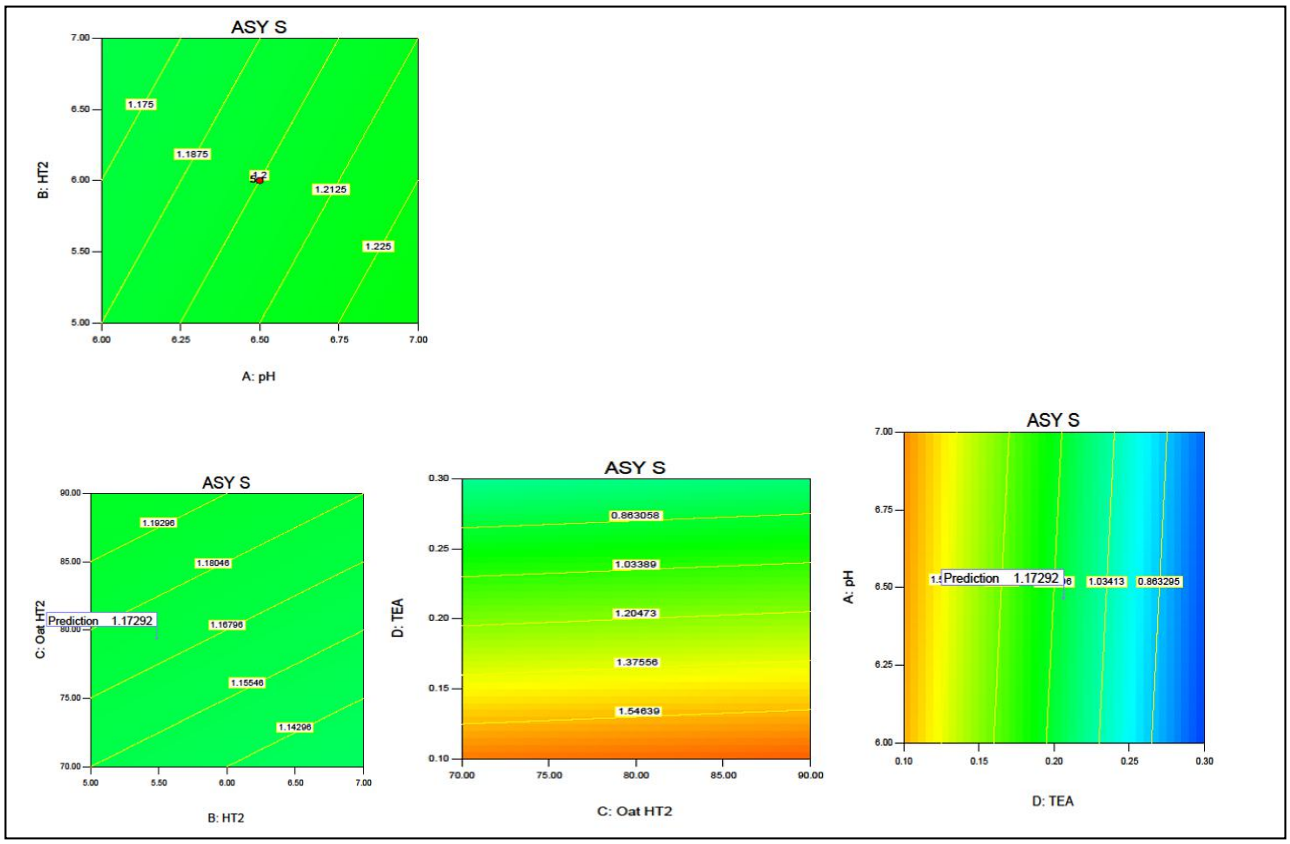

Figure 7.26 Contour plots for response asymmetry of VER

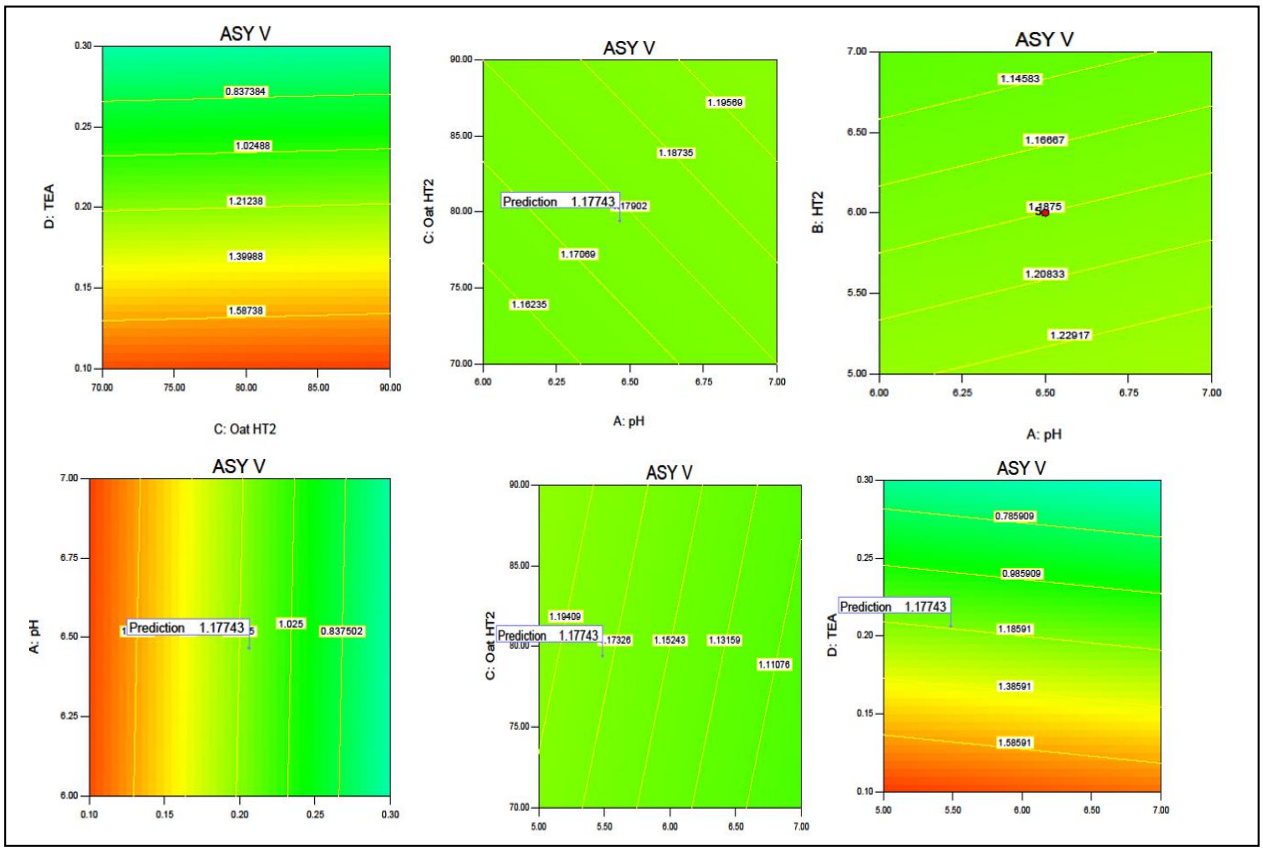

Figure 7.27 2D overlay plot showing the design space.

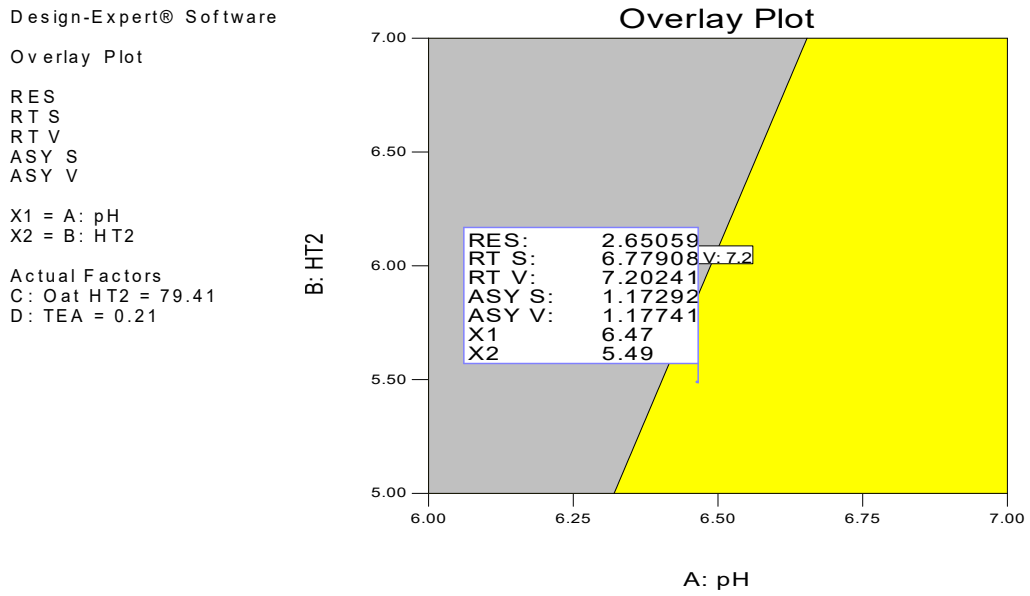

Figure 7.28 3D overlay plot showing the design space.

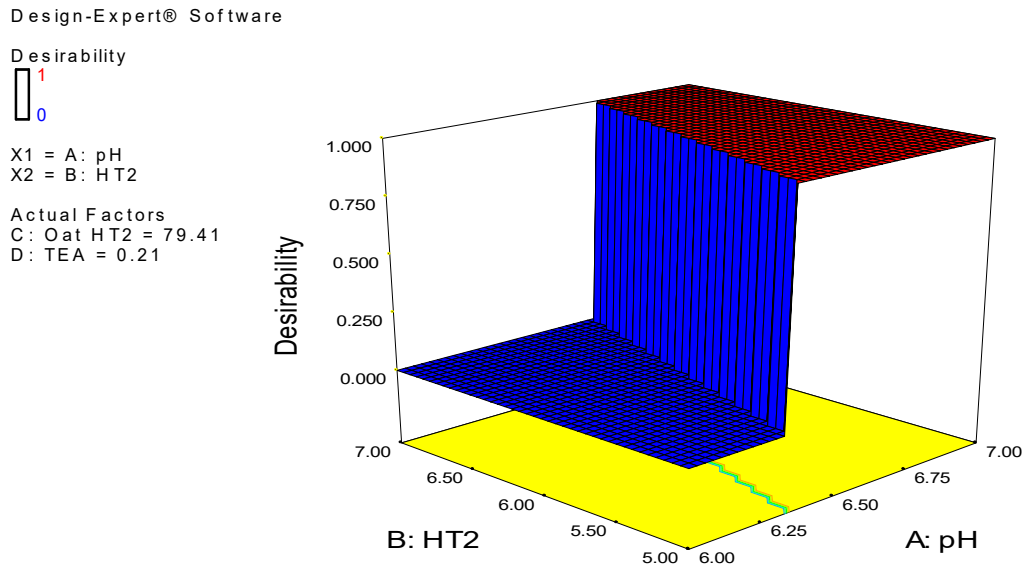

Figure 7.29. Derringer desirability plot.

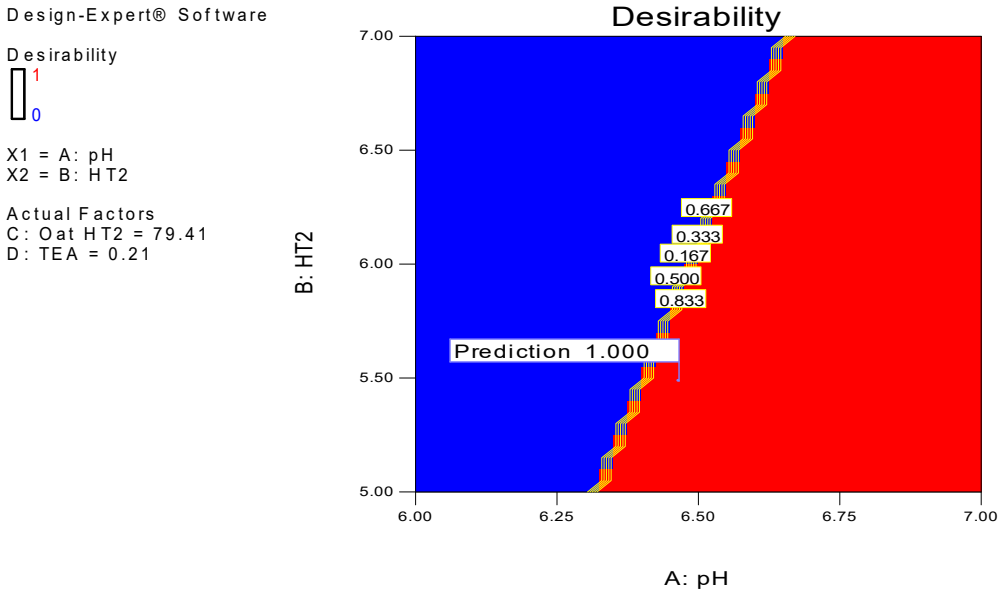

Table 7.5c Point verification and working point selection

Response	Prediction	Observed	95% CI-high	95% CI-low	SE Pred
Resolution	2.650575414	2.68	0.456057749	0.456057749	0.456057749
RT of SIL	6.779089643	6.74	0.129955382	0.129955382	0.129955382
RT of VER	7.202413168	7.35	0.163790755	0.163790755	0.163790755
Asy of SIL	1.172921195	1.21	0.115222186	0.115222186	0.115222186
Asy of VER	1.177427692	1.19	0.199481724	0.199481724	0.199481724

Confidence interval (95%) for the responses obtained from the selected working point

7.5.2.5 Chromatographic method optimization

A gradient chromatographic method was finalized falling in the design space. Mobile phase ratio of 65:35 (methanol: DDW added with 0.2% organic modifier TEA adjusted with formic acid for pH 6.5). The gradient elution followed (2min 65:35, 4min 75:25, 5.5min 80:20, 8min 65:35, 15min 65:35) scheme. The detection wavelength was set at 254 nm, flow rate was set as 1.0 ml/min, separation was achieved using Waters C_{18} (250 mm x 4.6 mm, 5 µm) column and the analysis was carried out at ambient temperature. The optimized peak in the chromatogram for SIL, VER, TAD, WFA, WDA was obtained at 4.0, 6.7, 7.3, 9.0, 11.3 min. The linearity range for analysis of SIL, VER, TAD, WFA, and WDA was obtained as 2-12 µg/ml. The developed HPLC method was validated as per ICH guidelinesThe optimized chromatogram having resolved peaks for the five components are shown in Figure 7.30. Also, overlay chromatogram is shown (Figure. 7.31) for the range 2-12 µg/ml for each of SIL, TAD and VER for quantitative analysis of these adulterants if added in the marketed formulations of Withanolides.

Figure. 7.30 Optimized chromatogram showing well resolved peaks of WDA, WFA, SIL, VER and TAD.

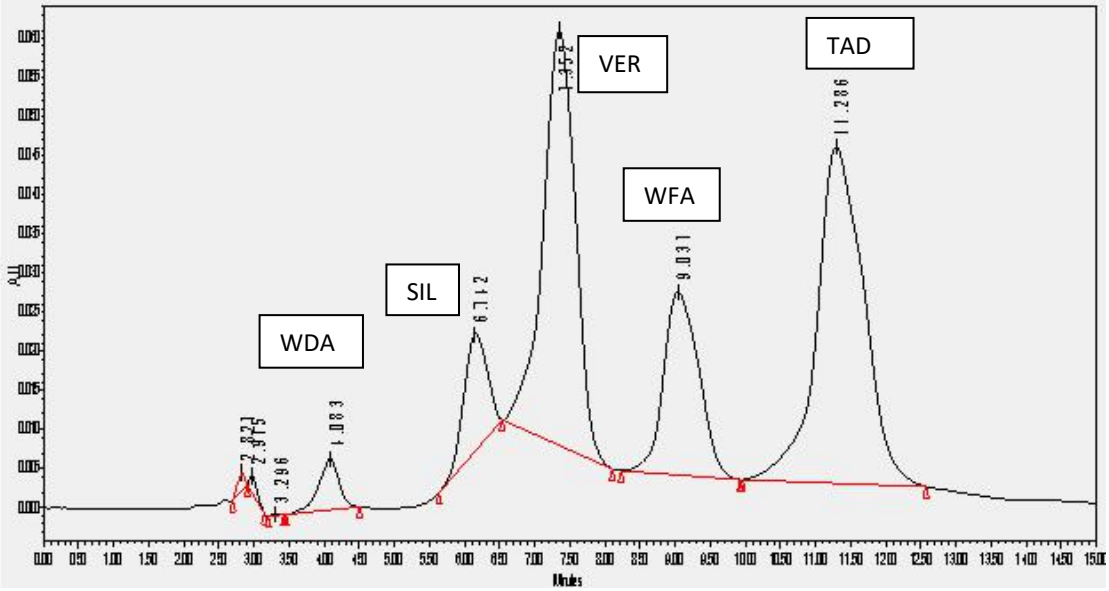

Figure. 7.31 Optimized overlay chromatogram showing for quantitative determination in range 2 - 12 µg/ml.

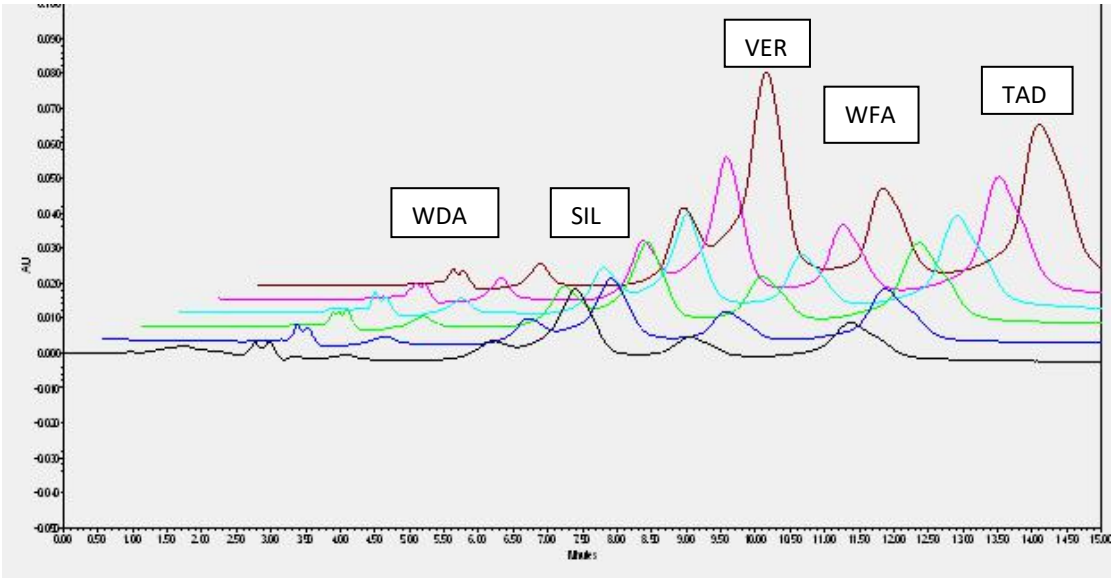

7.5.2.6. Method validation using ICH Q2 (R1) guideline

The developed HPLC method was validated as per ICH guidelines. The summary of validation parameters and system suitability parameters for developed chromatographic method is represented in Table 7.6.

Table 7.6 Summary of validation and system suitability parameters for developed chromatographic method.

Parameter (Units)	WDA	SIL	VER	WFA	TAD
Linearity range (µg/ml)	2-12	2-12	2-12	2-12	2-12
Correlation coefficient	0.9991±0.00482	0.9989±0.00129	0.9995±0.00332	0.9993±0.04725	0.9990±0.02981
Recovery (%)	99.85	100.30	99.48	101.34	100.56
Precision (%RSD)					
Interday (n=3)	0.48	0.35	0.83	0.36	1.02
Intraday (n=3)	0.64	0.58	0.27	0.83	0.63
Robustness	Robust	Robust	Robust	Robust	Robust
RT (min)	4.0±0.01	6.7±0.03	7.3 ±0.02	9.0 ±0.05	11.3±0.09
LOD (µg/ml)	0.23	0.44	0.25	0.45	0.42
LOQ (µg/ml)	0.70	1.32	0.77	1.35	1.30
Asymmetry	1.43	1.21	1.19	1.08	1.34
Theoretical plates	3013	2415	5147	8939	15208
Resolution	-	3.83	2.68	2.99	2.83

RSD-Relative standard deviation, SST- System suitability test parameters, Retention time-RT

7.5.2.7 Application of developed method for differentiating between counterfeit, placebo and marketed samples

The ultimate aim of the study was to detect the counterfeiting if added as adulterant in Withania somnifera herbal formulation. Ashwagandha powder formulation was taken as an ideal sample to study the adulteration. For that 1 gm Ashwagandha powder was taken in 10 ml methanol. It was then refluxed for 5 hours at 80°C, sonicated and centrifuged for 15 min each respectively. The supernatant thus formed was collected and injected into the chromatographic system for each formulation. Using the optimized method, analysis was undertaken of 6 marketed formulations coded as FM1 to FM6, 4 placebo samples coded as PL1 to PL4 and 5 counterfiet samples coded as CF1 to CF5. The formula for preparation of CF as well as PL samples is shown in Table 7.7. None of the marketed formulations of Withania sominfera showed the peaks of probable adulterants SIL, VER and TAD. The placebo samples did not show peaks of WDA, WFA as well as SIL, VER and TAD. However, the laboratory prepared counterfeit samples showed peaks of deliberately added counterfeits for analysis if at all found in real world samples as shown in Figure.7.30. Though all the commercial Ashwagandha formulation did not show any adulteration, the LOD and LOQ values of developed method indicate the high sensitivity of the

developed method and would be a good tool to assess the counterfeit drugs if any are added to ashwagandha formulation.

Table 7.7 Formulation summary for CF and PL samples.

Samples taken	Quantity (mg)				
	CF1	CF2	CF3	CF4	CF5
Standard Ashwagandha root powder	20	20	20	20	20
SIL	10	-	-	10	10
TAD	-	10	-	10	10
VER	-	-	10	10	-
Lactose	20	20	20	-	10

Excipients taken	Quantity (mg) per 650 mg tablet			
	PL1	PL2	PL3	PL4
Lactose	500	507	497	509
Talc	6	6	6	6
Magnesium stearate	6	6	6	6
Cross povidone	6	6	6	6
Starch	132	125	135	123

7.6 SECTION –B

7.6.1 Experimental

Development of chemometric assisted analytical method for checking adulteration of Sildenafil citrate, Verdenafil, Tadalafil in Ashwagandha herbal tablets using NIR, Raman and ATR data

7.6.1.1 Chemicals and materials

All chemicals and materials required for this study were procured and used as mentioned in section 7.5.1.1.

7.6.1.2 Equipments and analysis conditions

IR-Affinity Fourier Transform infrared (FTIR) spectrometer, Shimadzu, was used for FTIR analysis equipped with IR solution software. The samples were analyzed by Miracle 10 single reflection attenuated total reflectance accessory.
The NIR analysis was carried out by Thermo Scientific NIR, micro-PHAZIR RX Analyzer equipped with Method Generator software version 4. The Raman spectroscopy was performed on STR Raman Spectrometer, AIRIX CORP and the data processing was carried out with gramsIQ software and Origin software.
The Raman signals were detected using high resolution CCD detector. For chemometrics, Minitab 10.0 version was used for the data processing and analysis. All recorded spectra were background corrected. PCA and HCA techniques were applied to the spectral data.

7.6.1.3 Sample preparation and analysis by various Spectroscopic methods

For spectroscopic analysis, the total fifteen samples to be analysed comprised of six commercial formulation (FM) samples coded as LN, GD, HM, AF, CN and GH, five laboratory prepared counterfeit (CF) samples coded as CF1, CF2, CF3, CF4, CF5 and four placebo (PL) samples coded as PL1, PL2, PL3, PL4. The formulation summary for PL and CF samples was as presented in Table 7.7.The CF samples were weighed as per the quantity given in table 7.7 and then mixed uniformly using mortar and pestle and then used for the analysis. For PL samples also the powder samples were weighed as per the quantity given in table 7.7 and then geometric mixing of powders was conducted using mortar pestle for uniform distribution of powders for analysis. [13]

For FTIR analysis the powdered samples were directly put under the ATR probe and analysed. The powdered samples of counterfeit and placebo samples were analysed in a similar way. All samples (counterfeit, original and placebo) for each drug were first measured by the FTIR. The scan covered the range (4000-600cm-1) nm (about 2 nm increments). The spectrum of each sample was an average of five scans. A matrix of 15×1763 (15 samples and 1763 wavelengths) (Figure 7.32) was formed which was subjected to chemometric modelling.

For NIR analysis, the tablet formulations, which were to be analysed, were powdered, filled in a polythene bag. 100 mg of powder mixture was taken, spread over the previously marked area of 1 cm^2 on the polythene bag and were analysed. The samples were then measured by NIR. The scan covered the range (1600-2400cm^{-1}) at about 8 nm increments. The spectrum of each sample was an average of five scans. A matrix of was 15×100 (15 samples and 100 wavelengths) (Figure 7.33) was formed in study which was subjected to chemometric modelling.

For Raman analysis, the powdered samples were spread on a glass slide and kept on the stage of microscope and analysed. The samples were analysed by Raman spectrometer using a laser of 785 nm wavelength for excitation. The Raman signals scanned over a range of 700-1800 cm^{-1} Raman shift with 30 seconds of integration time. The spectrum of each sample was an average of ten scans. A matrix of 15×1100 (15 samples and 1100 wavelengths) (Figure 7.34) was formed in study which was subjected to chemometric modelling.

7.6.1.4 Chemometrics

Every drug formulation has a unique spectral fingerprint in the NIR, Raman and IR spectra that identifies the brand of the drug. Chemometrics provides multivariate model which can highlight the slightest difference in the spectral features of drug. Incorrect formulations containing foreign or substitute ingredients can put the patient's life under risk. Taking this basic concept to compare the entire spectra, PCA and HCA chemometric techniques were used to detect fine differences in the spectra. [26]

7.6.1.4.1 PCA

The PCA works on the principle that it finds the directions (or vector) in the space of data along which the dispersion (or variance) of the data is maximum. The directions or vectors are called principle components (PCs). The PCs are calculated in such a way that the first PC carries majority or maximum information which is statistically termed as "Explained variance". The second PC is thus calculated and carries maximum information or variance that has not been included by the first PC. Similarly the PC's are further calculated (PC3, PC4 and so on) till all the information of the data has been accounted. The two PCs which explain most of the variance are selected for building the PCA model. In predicting PCA score plots, samples that form a cluster are believed to belong to the same origin. Each one of the groups of samples represents certain similarity and for the present study it represented similar form of the samples (counterfeit, original and placebo) [27].

7.6.1.4.2 HCA

For further investigation of the samples, hierarchical cluster analysis (HCA) was also used. The Ward error sum of squares hierarchical clustering method was used for the study. The clustering by Ward's method is based on minimum variance. The results by HCA are obtained in form of dendograms which measures euclidean distance based on Ward linkage.

7.6.1.4.3 Satitzky-Golay derivative

Savitzky-Golay is used for calculating smoothing and differentiation of data by least-squares technique. The Savitzky-Golay approach has been widely used because it produces a significant improvement in the lengthy least-squares calculation by making a simple and equivalent, convolution. In this approach the least-squares value of a given point is calculated as a weighted combination of itself and m points on either side of it. This corresponds to performing moving (2m + 1 point) least-squares fit across the data. [28,29]

7.6.2 Results and discussion

7.6.2.1 Sample analysis using NIR, Raman and ATR

For spectroscopic studies, analysis of total 15 samples was carried out as discussed above. Their FTIR, NIR and Raman spectroscopic analysis were carried out as described by procedure under the methodology. The overlay spectra of all 15 samples of FTIR, NIR and Raman spectroscopic analysis by zero order were obtained as represented in Figure 7.32 to 7.34.

Figure 7.32 FTIR overlay (zero order) plot of matrix (15 samples X 1763 wavelengths)

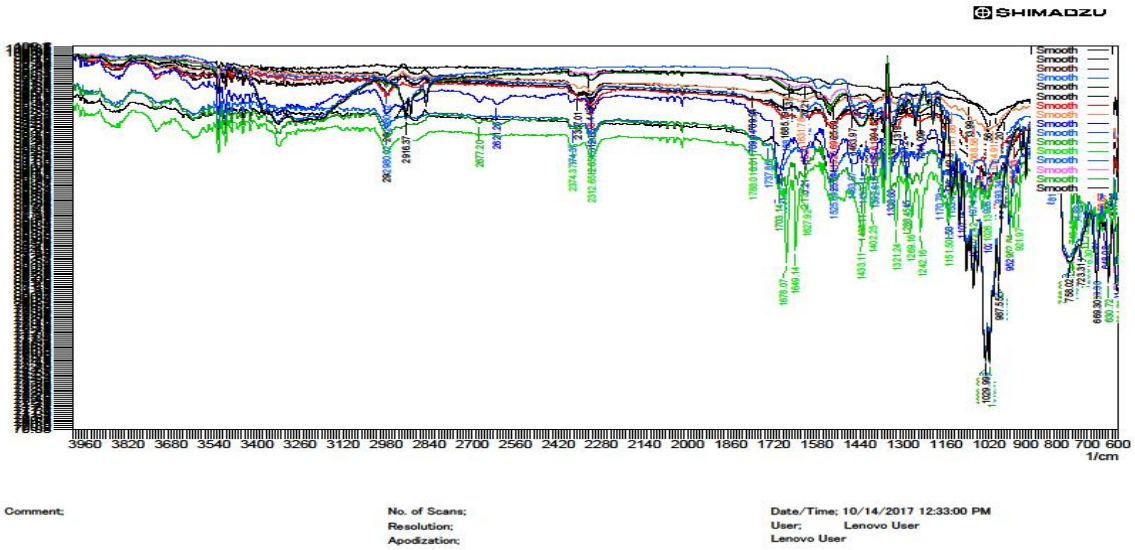

Figure 7.33 NIR overlay (zero order) plot of matrix (15 samples X 100 wavelengths)

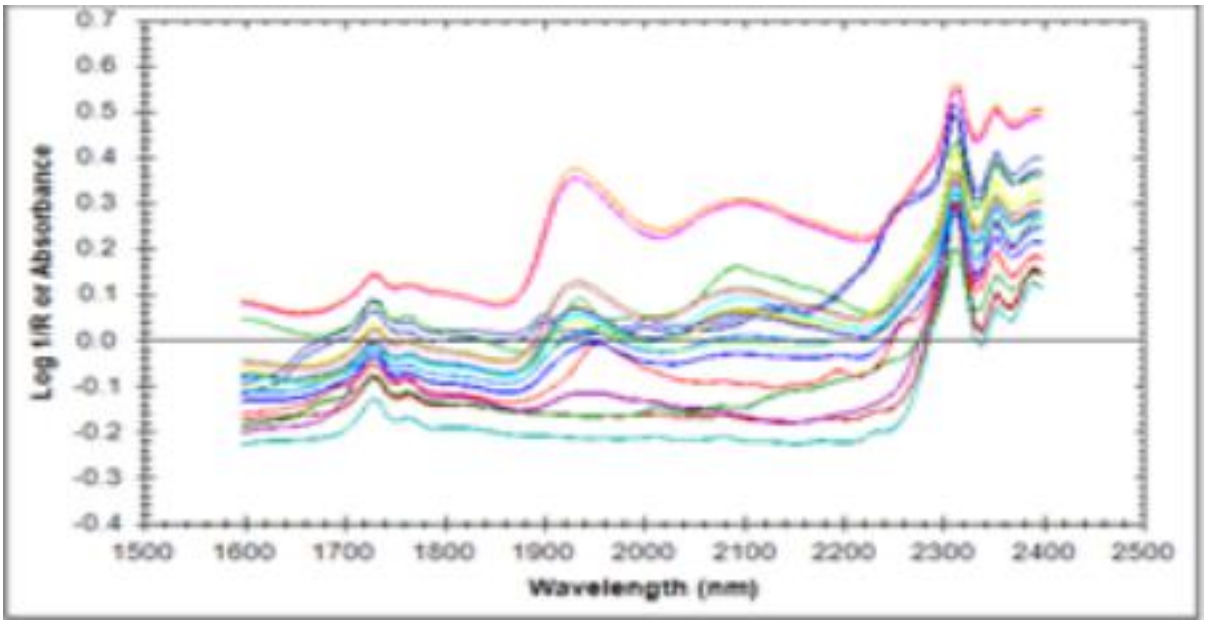

Figure 7.34 Raman overlay (zero order) plot of matrix (15 samples X 1100 wavelengths)

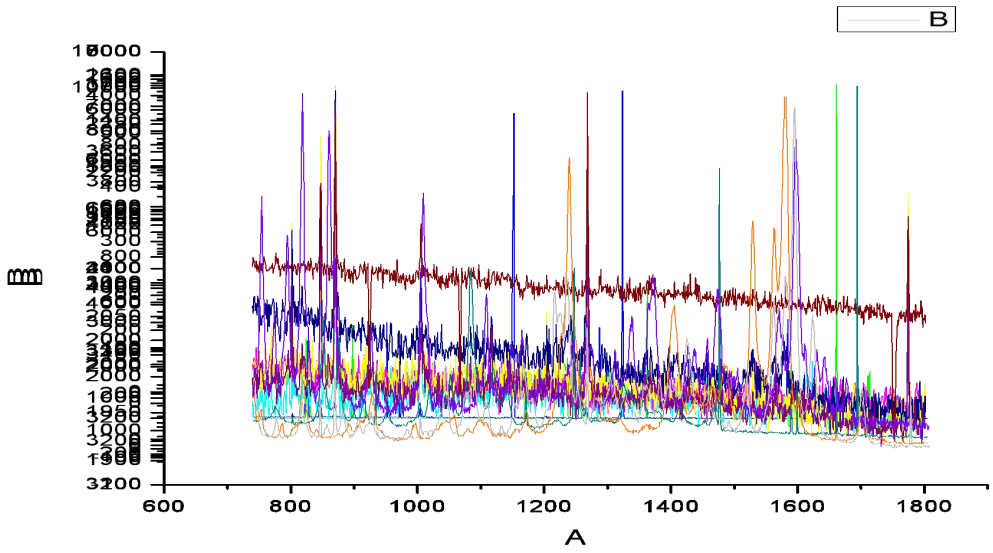

7.6.2.2 Statistical analysis by chemometrics techniques like PCA and HCA

The Exploratory data analysis (EDA) utilizing the chemometric techniques such as Principal component analysis (PCA) and Hierarchical cluster analysis (HCA), which reduce large complex data sets to simplified and interpretable views were applied. These views highlight the natural groupings in the data and show which variables most strongly influence those patterns. These techniques prove to be very powerful tool for discrimination and counterfeit study with respect to the original or reference sample. The PCA technique was combined with hierarchical cluster analysis to establish an automated approach for the discrimination between different groups of FM, CF and PL samples.

In Figure 7.35 representing PCA plot for zero order Raman data, 3 clusters can be distinguished, each for placebo, counterfeit as well as formulation samples. Also in Figure 7.36, HCA plot for zero order Raman data, 3 clusters in the dendogram can be seen where the euclidean distance is less in between clusters representing the same type of samples waiving few exceptions where minor differences in distance between groups is not distinguished.

Figure 7.35 PCA plot for zero order data of Raman spectroscopy

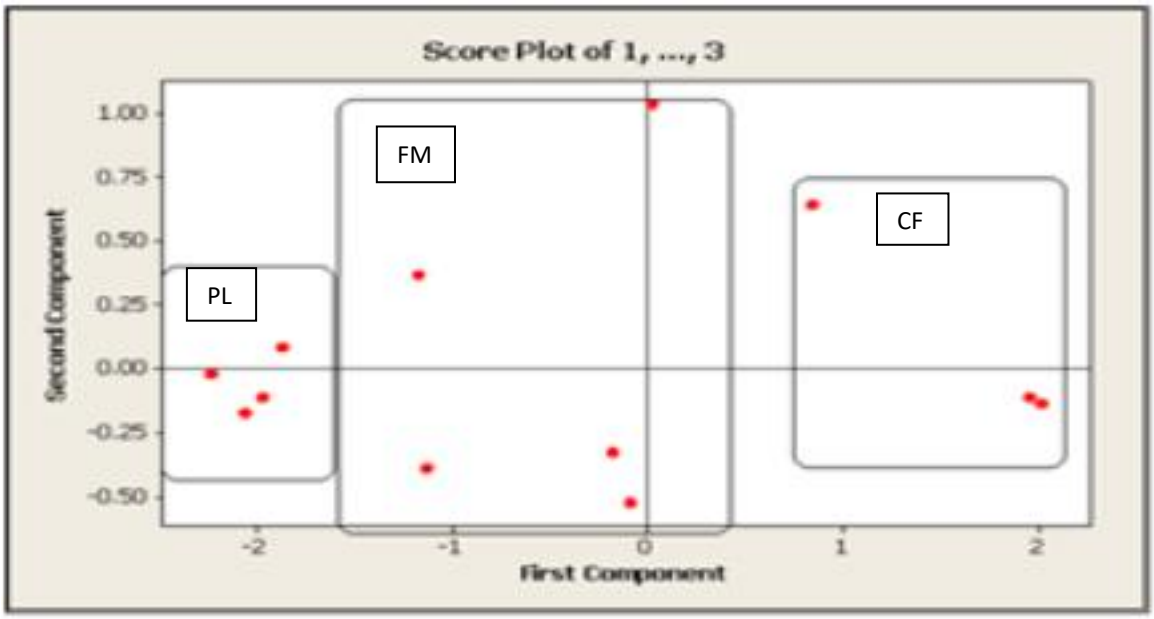

Figure. 7.36. HCA plot for zero order data of Raman spectroscopy

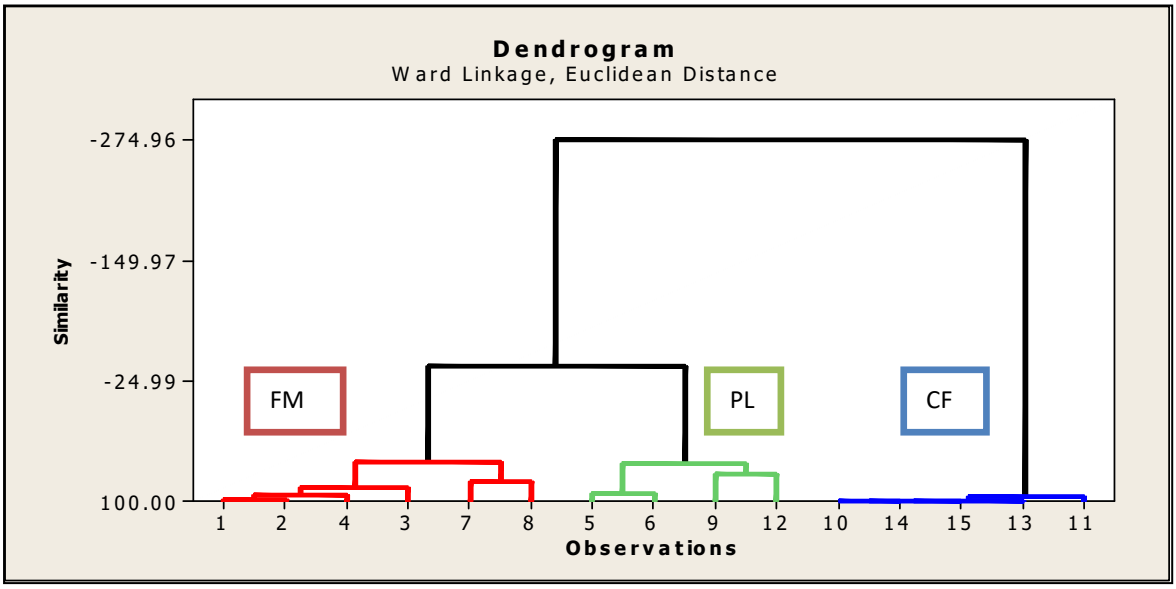

Similarly in Figure 7.37 representing PCA plot for zero order FTIR data and in Figure 7.38 representing HCA plot for zero order FTIR data, 3 clusters, each for placebo, counterfeit as well as formulation samples are clearly formed where the euclidean distance is less inbetween clusters representing the same type of samples waiving few exceptions where minor differences in distance between groups is not distinguished.

Figure 7.37. PCA plot for zero order data of FTIR spectroscopy

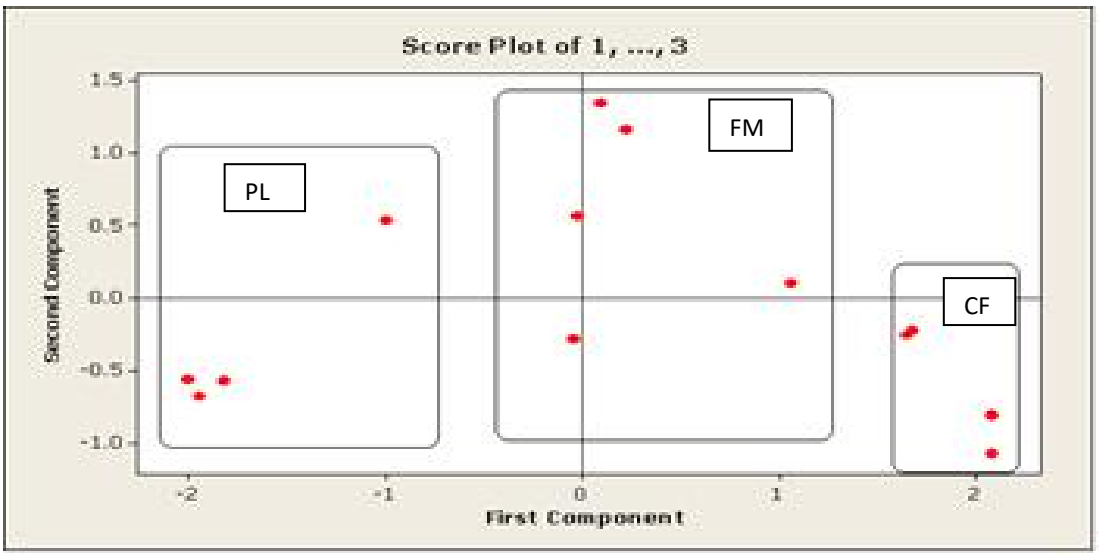

Figure. 7.38. HCA plot for zero order data of FTIR spectroscopy

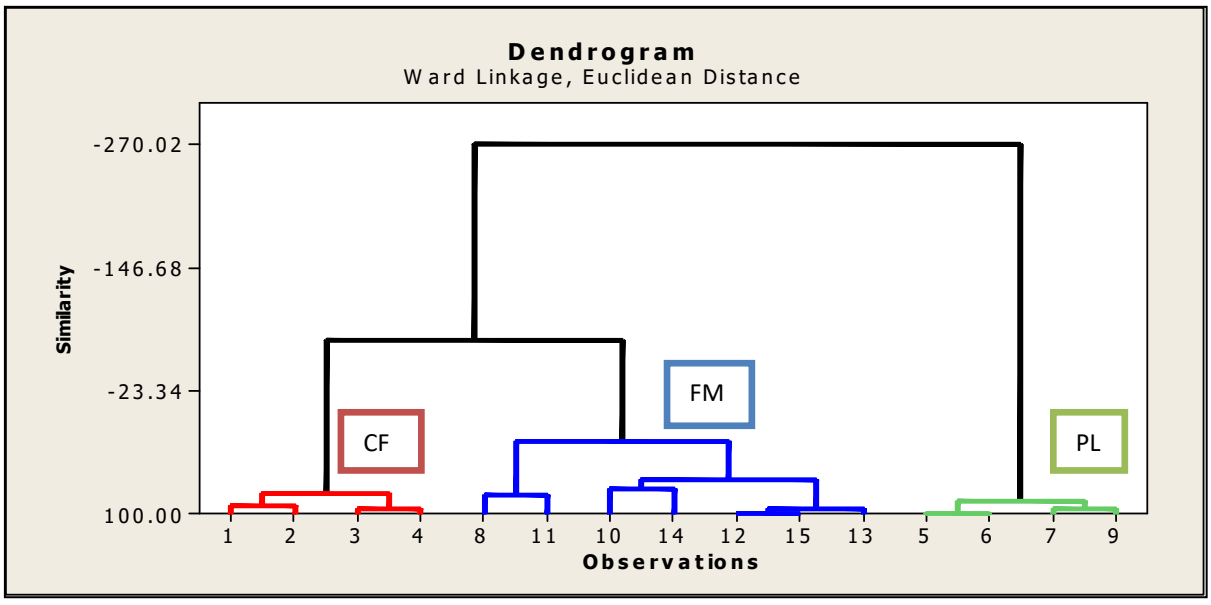

The three clusters which were clearly differentiated by Raman and FTIR spectroscopy are somewhat overlapping in PCA and HCA plots (Figure 7.39 and Figure 7.40) for zero order NIR spectroscopy also.

Figure. 7.39. PCA plot for zero order data of NIR spectroscopy

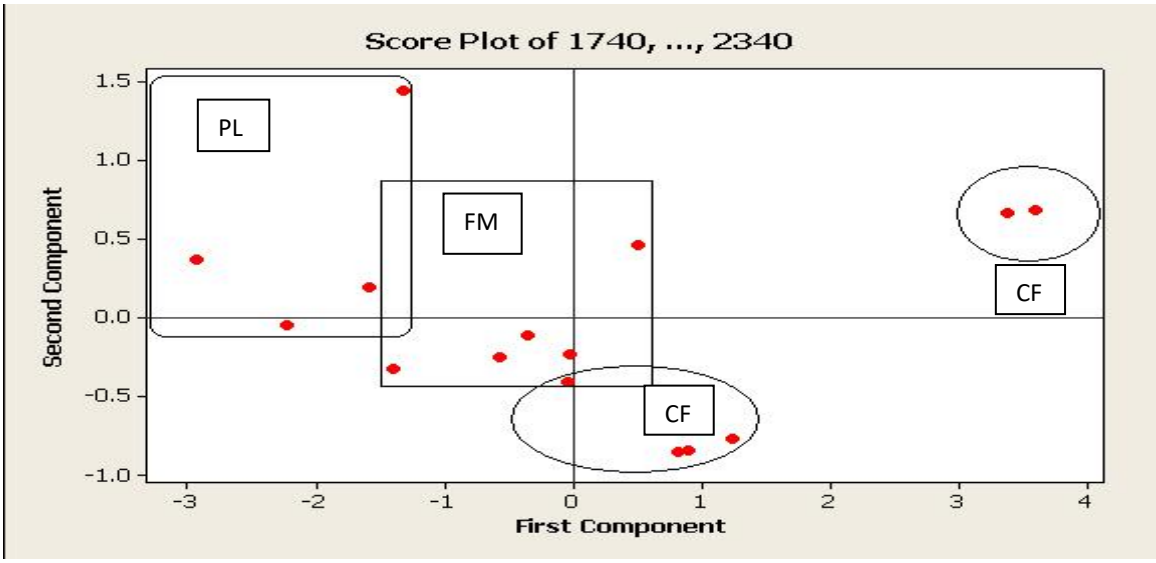

Figure 7.40. HCA plot for zero order data of NIR spectroscopy

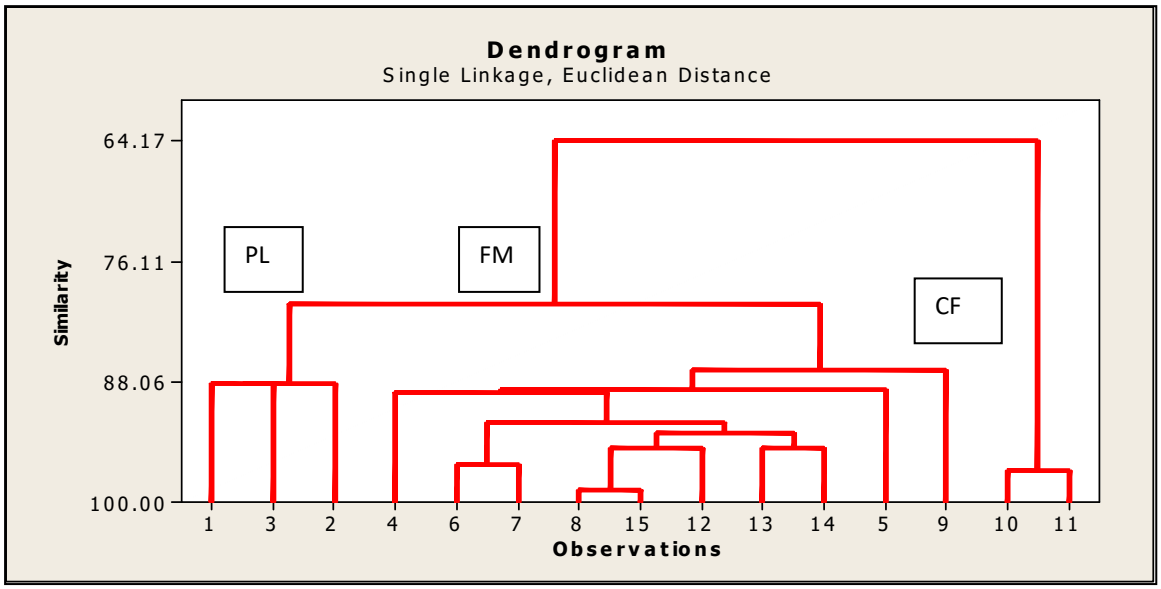

For zero order FTIR as well as Raman data similar pattern was observed in PCA as well as HCA plots. As, placebo samples consists of same excipients with only a minor variation in quantity of lactose for PL1 to PL4, we can see them clustered together in PCA plot. We consider first component in PCA having having >99% information about the data thus PL samples occur on the negetive side and CF sampless appear on the positive side whereas FM samples are scattered around the neutral region. In HCA plots, PL1 to PL4 samples have minor differences in Euclidean distance and thus leads to ward linkage in the dendogram. For formulation samples coded as LN, GD, HM, AF, CN, GH, the cluster is scattered as compared to placebo samples. The pattern shows appearance of points for HM sample distant from other formulations also the point for LN sample is somewhat distant from the cluster of all other 4 formulations coded as CN, GD, GH and AF. Similarly in HCA plots for LN, GD,

HM, AF, CN, GH samples very minor differences in Euclidean distance is observed and thus leads to ward linkage in the dendogram. For counterfeit samples coded as CF1 to CF5, also the cluster is scattered and the points distant from the cluster are for TAD containing CF samples (CF2, CF4 and CF5) as its chemical struture is having major variations compared to SIL and VER chemical structure. Refer Figure 7.1, Figure 7.2 and Figure 7.3 for chemical structure of SIL, VER and TAD. Similarly in HCA plots for CF1 to CF5, samples have minor differences in Euclidean distance and thus lead to ward linkage in the dendogram. Whereas for zero order NIR data it was observed that the clusters are not stacked properly and show random distribution of points as compared to FTIR and Raman data. Considering the first component, points for placebo samples coded as PL1 to PL4 are stacked on negetive side whereas point for CF samples coded as CF1 to CF5 are randomly scattered on positive side. In CF samples, points for CF2, CF4 and CF5 are nearing zero whereas points for CF1 and CF3 are on extreme positive side due to absence of TAD in it. The FM samples are scattered around neutral region in which the HM sample is away from other stacked samples towards positive side and LN sample is also somewhat distant from stacked samples towards negetive side. In HCA plot of NIR data, due to presence of scattered data, no ward linkage is observed. Thereby, we have to conclude only on basis of Euclidean distance. The samples having minor variation in Euclidean distance are from similar group. As evident from the figure 7.40, first group in the dendogram is for PL samples, second group is for FM samples as well as third group is for CF samples.

7.6.2.3 Application of Savitzy Golay derivatization for chemometrics techniques like PCA and HCA

Derivatization often enhances the spectral differences; the PCA and HCA therefore were also performed by applying the Savitzky-Golay derivative method. The first derivative algorithm was applied to the normal zero order spectra by using SGolay algorithm (Figure 7.41 for FTIR data, Figure 7.42 for NIR data) and the second derivative algorithm was applied to the normal zero order spectra by using SGolay alogorithm. (Figure 7.43 for Raman data) and then PCA and HCA were performed.

Figure 7.41. FTIR overlay (SGolay first order) plot of matrix (15 samples X 1763 wavelengths)

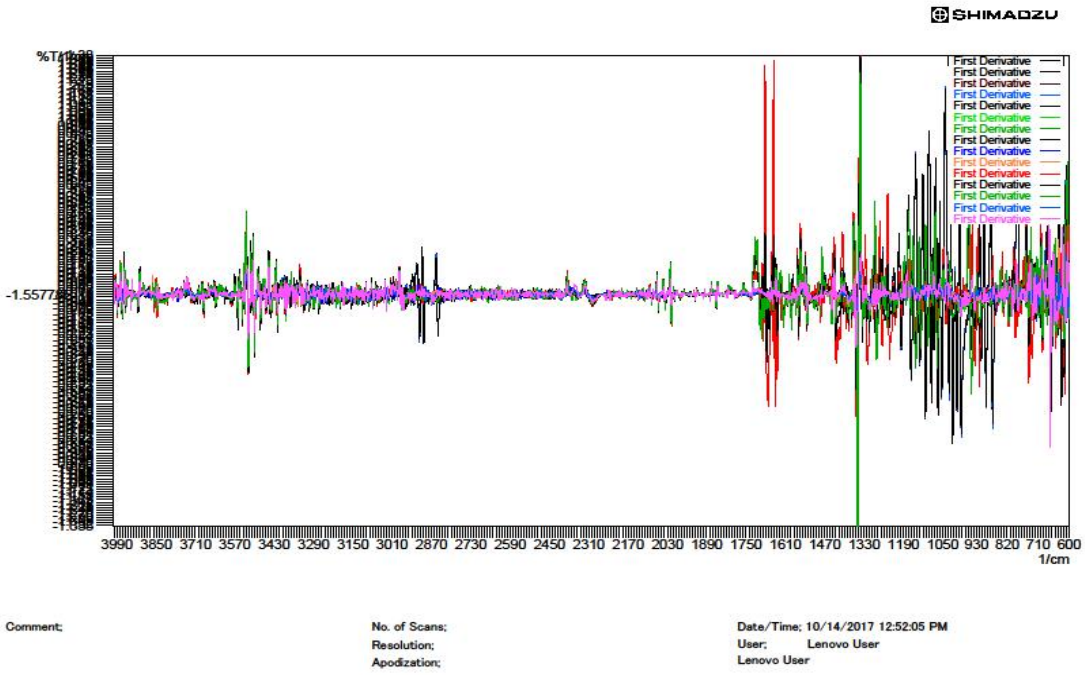

Figure 7.42. NIR overlay (SGolay first order) plot of matrix (15 samples X 100 wavelengths)

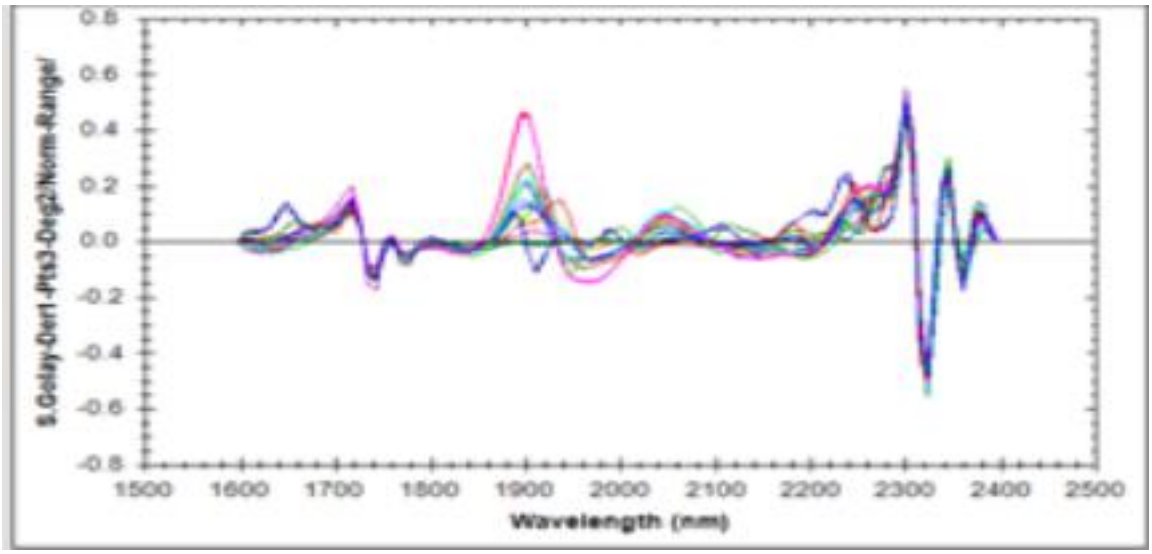

Figure 7.43. Raman overlay (SGolay second order) plot of matrix (15 samples X 1100 wavelengths)

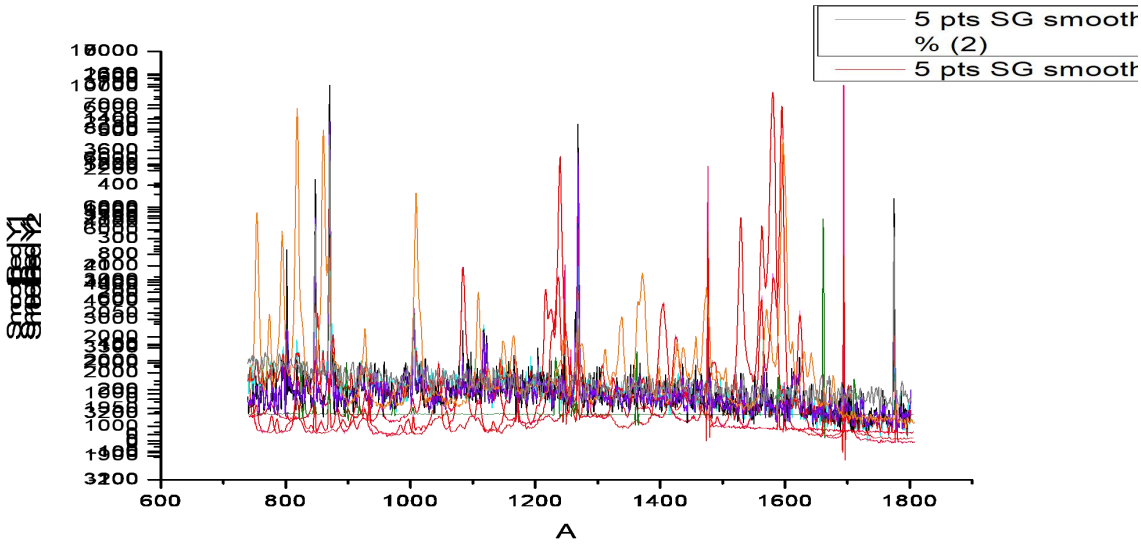

In Figure 7.44 and Figure 7.45 representing PCA and HCA plot respectively for second order derivative Raman data we can distinguish 3 clusters, each for placebo, counterfeit as well as formulation samples more clearly. In HCA plot euclidean distance is less inbetween clusters representing only the same type of samples.

Figure 7.44. PCA plot for second order SGolay derivative data of Raman spectroscopy

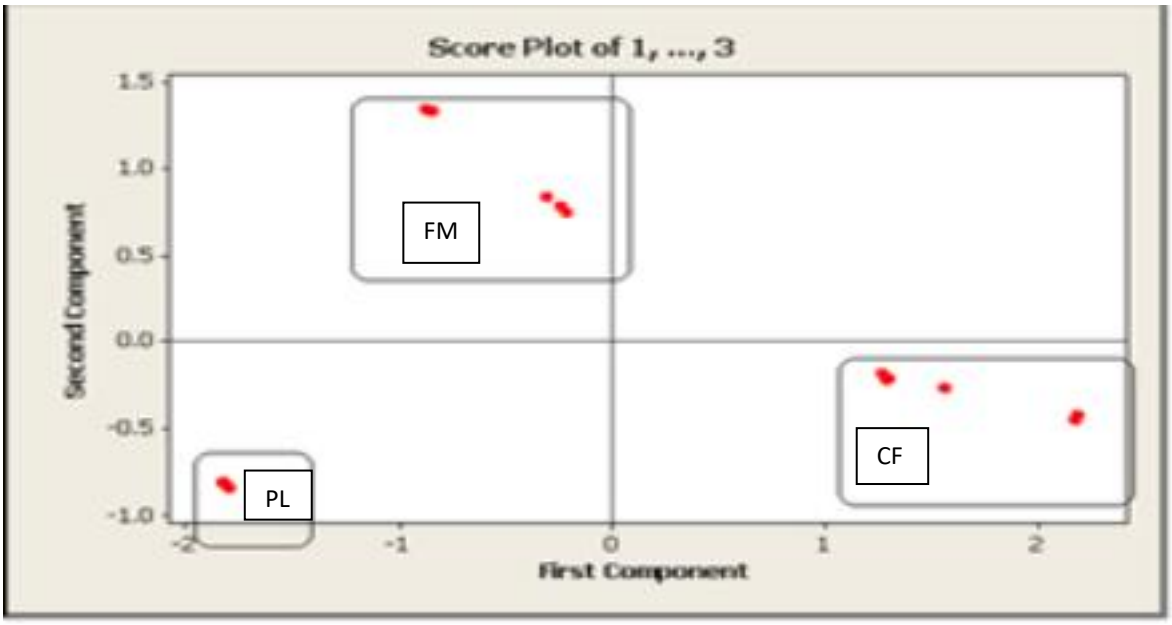

Figure. 7.45 HCA plot for second order SGolay derivative data of Raman spectroscopy

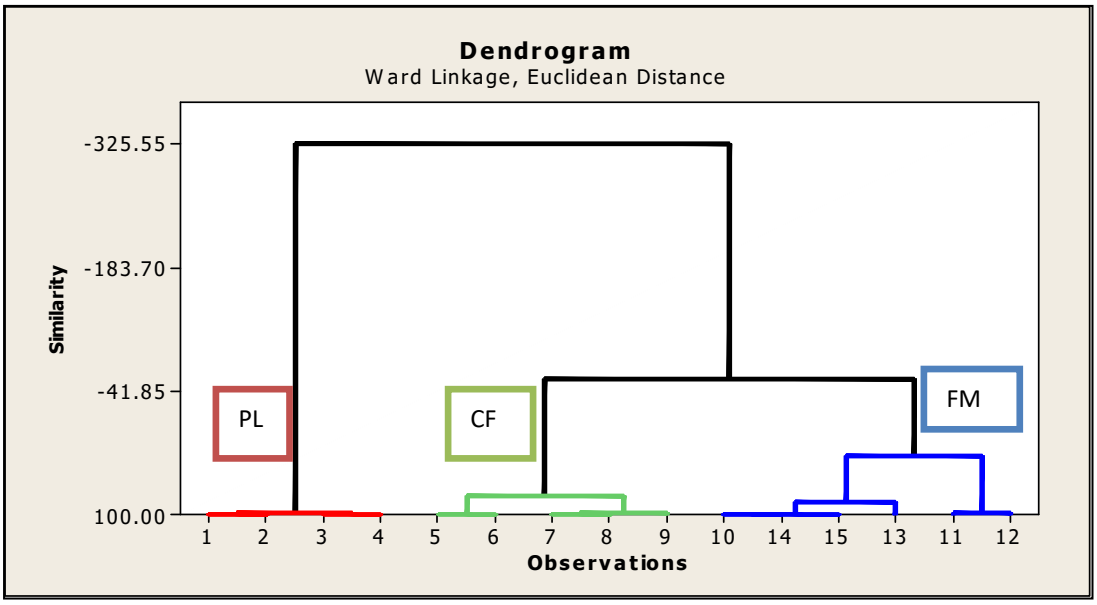

In Figure 7.46 and Figure 7.47 representing PCA and HCA plot respectively for first order derivative FTIR data, we can distinguish 3 clusters, each for placebo, counterfeit as well as authentic Withania somnifera marketed formulations clearly. In HCA plot the euclidean distance is less inbetween clusters representing the same type of samples waiving few exceptions where minor differences in distance between groups is not distinguished.

Figure. 7.46. PCA plot for SGolay first order derivative data of FTIR spectroscopy

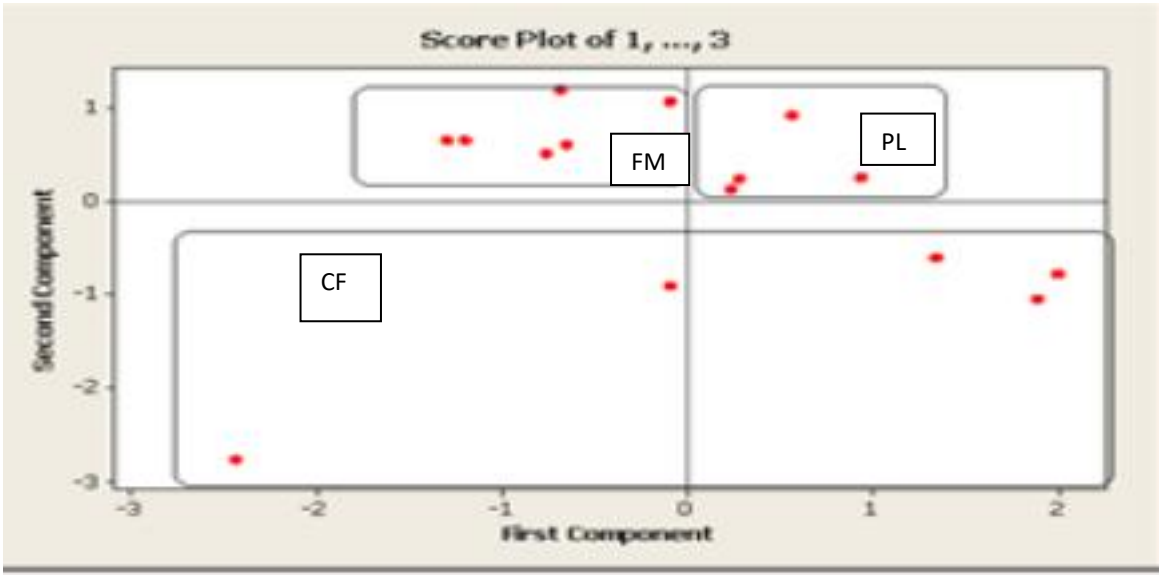

Figure. 7.47. HCA plot for SGolay first order derivative data of FTIR spectroscopy

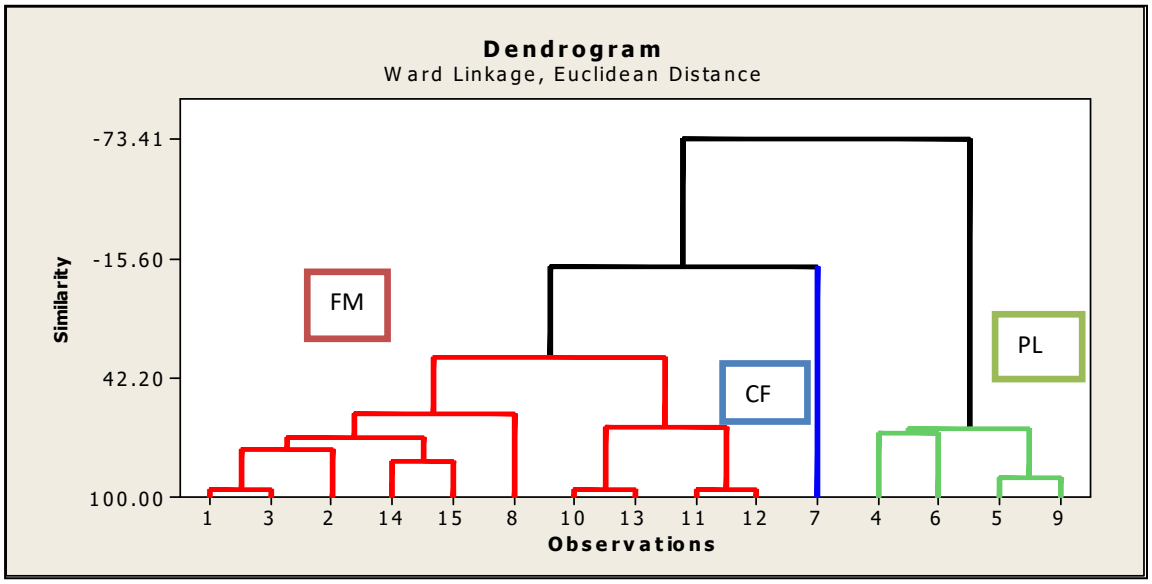

In Figure 7.48 and Figure 7.49 representing PCA and HCA plot respectively for first order derivative NIR data, we can distinguish 3 clusters, each for placebo, counterfeit as well as authentic Withania somnifera marketed formulations clearly. In HCA plot the euclidean distance is less inbetween clusters representing the same type of samples waiving few exceptions where minor differences in distance between groups is not distinguished.

Figure 7.48. PCA plot for SGolay first order derivative data of NIR spectroscopy

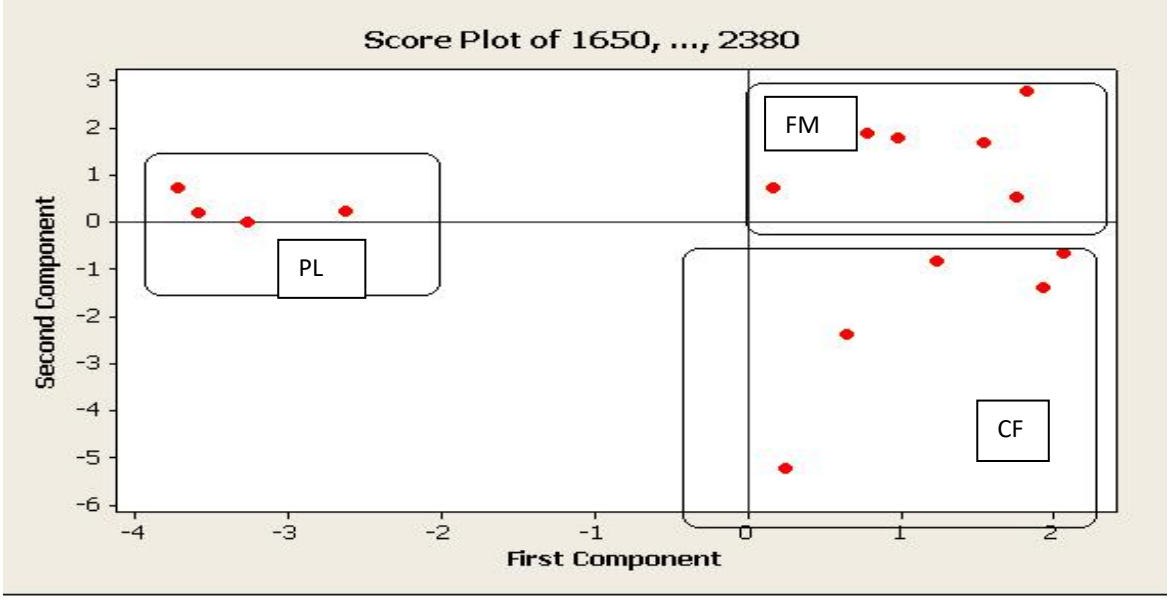

Figure 7.49. HCA plot for SGolay first order derivative data of NIR spectroscopy

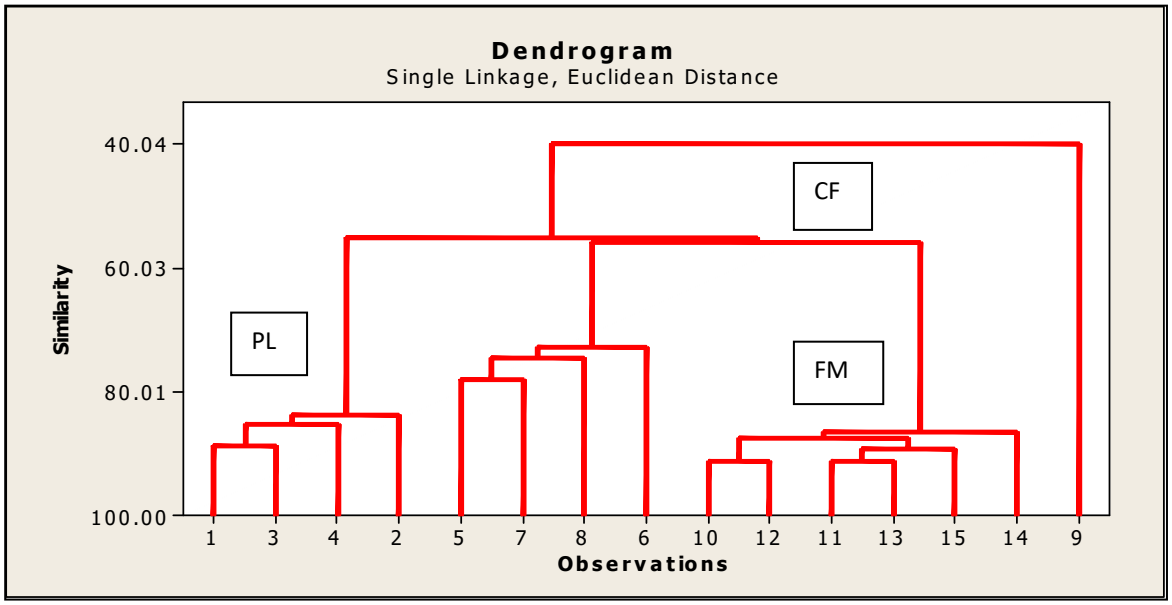

For second order SGolay derivative of Raman data, also as placebo samples consists of same excipients with only a minor variation in quantity of lactose for PL1 to PL4, we can see them clustered together in PCA plot. For derivative data we consider second component in PCA having having >99% information about the data thus PL and CF samples occur on the negetive side and FM sampless appear on the positive side. In HCA plots, PL1 to PL4 samples have minor differences in Euclidean distance and thus leads to ward linkage in the dendogram. For formulation samples coded as LN, GD, HM, AF, CN, GH, the cluster is scattered as compared to placebo samples. The pattern shows appearance of points for HM and LN sample distant from other 4 formulations coded as CN, GD, GH and AF. Similarly in HCA plots for LN, GD, HM, AF, CN, GH samples very minor differences in Euclidean distance is observed and thus leads to ward linkage in the dendogram. For counterfeit samples coded as CF1 to CF5, also the cluster is scattered and the points distant from the cluster are for TAD containing CF samples (CF2, CF4 and CF5) as its chemical struture is having major variations compared to SIL and VER chemical structure. Refer Figure 7.1, Figure 7.2 and Figure 7.3 for chemical structure of SIL, VER and TAD. Similarly in HCA plots for CF1 to CF5, samples have minor differences in Euclidean distance and thus lead to ward linkage in the dendogram. Whereas for first order FTIR data it was observed that the clusters are not stacked properly and show random distribution of points as compared to Raman data. Considering the second component, points for PL and CF samples are stacked on positive side whereas point for FM samples are randomly scattered on negetive side. In CF samples, as per the first component points for CF2, CF4 and CF5 are on positive side whereas points for CF1 and CF3 are on negetive side due to absence of TAD in it. Similarly in HCA plots for CF1 to CF5, samples have minor differences in Euclidean distance and thus lead to ward linkage in the dendogram. The FM samples are scattered on positive side as per second component in which the HM and LN sample is away from other stacked samples. In HCA plots for

LN, GD, HM, AF, CN, GH samples very minor differences in Euclidean distance is observed and thus leads to ward linkage in the dendogram.In HCA plot of FTIR data, PL1 to PL4 samples have minor differences in Euclidean distance and thus leads to ward linkage in the dendogram.due to presence of scattered data, no ward linkage is observed. Whereas for first order NIR data it was observed that the clusters are not stacked properly and show random distribution of points as compared to Raman data. Considering the second component, points for formulations samples coded as LN, HM, CN, GD, AF, GH are stacked on positive side whereas point for CF samples coded as CF1 to CF5 are randomly scattered on negetive side. The placebo samples coded as PL1, PL2, PL3 and PL4 are scattered around the neutral region. In HCA plot of first order Sgolay NIR data, PL1 to PL4 samples have minor differences in Euclidean distance and thus lead to ward linkage in the dendogram. In CF samples, points for CF2, CF4 and CF5 are nearing zero whereas points for CF1 and CF3 are on negetive side due to absence of TAD in it. Similarly in HCA plots for CF1 to CF5, samples have minor differences in Euclidean distance and thus lead to ward linkage in the dendogram. The FM samples are stacked around positive side. Similarly in HCA plots for LN, GD, HM, AF, CN, GH samples very minor differences in Euclidean distance is observed and thus leads to ward linkage in the dendogram.

7.6.2.4 Summary of statistical analysis by chemometrics

A more clear distinction between different groups of samples was obtained by derivatizing the data. After derivatizing also most distinguished clusters were obtained by second order derivative Raman data. Also, a considerable distinction was obtained from FTIR data by zero as well as first derivative. Zero order NIR data, did not prove to be a very good model for distinguishing the different groups of samples, whereas first order model of NIR data, showed considerably satisfactory results. The first two principal components were considered for development of models, the explained variance for each data source viz Raman, NIR as well as FTIR for zero order and derivative data are represented in Table 7.8. The models thus developed can be easily applied for real world samples.

Table 7.8 Explained variance by first two principal components

Data source	Explained variance
Zero order NIR	95.80
First order derivative SGolay NIR	99.50
Zero order FTIR	87.10
First order derivative SGolay FTIR	97.10
Zero order Raman	94.40
Second order derivative SGolay Raman	98.70

7.7 CONCLUSION

By combination of chromatographic and spectroscopic analysis, a detailed analytical profile for distinction of counterfeit, placebo and marketed authentic samples of Withania somnifera was established. The CNX and DOE based chromatographic method provided a considerable design space for qualitative and quantitative analysis of deliberately added adulterants of synthetic analogues that is SIL, VER and TAD in standard withania somnifera samples. The spectroscopic analysis was able to implicate satisfactory distinction between the CF, FM and PL samples. Raman spectroscopic analysis along with data manipulation by conducting Savizky Golay second order derivatization proved to be best method for clear distinction between the three different groups of samples in comparison to other spectroscopic analysis carried out in our study. The chromatographic as well as spectroscopic analytical profile thus developed can be easily extended for real world samples and thus provide a thorough testing profile for analysis of counterfeits if any found in Withania Somnifera authentic samples.

7.8 REFERENCES

1. Yang YJ, Song DM, Jiang WM, Xiang BR. Rapid Resolution RP-HPLC-DAD Method for Simultaneous Determination of Sildenafil, Vardenafil, and Tadalafil in Pharmaceutical Preparations and Counterfeit Drugs. Analytical Letters. 2010; 43 (3): 373-80.
2. Zhang Y, Huang Z, Ding L, Yan H, Wang M, Zhu S. Simultaneous determination of yohimbine, sildenafil, vardenafil and tadalafil in dietary supplements using high-performance liquid chromatography-tandem mass spectrometry.J Sep Sci. 2010; 33 (14):2109-2114.
3. Zhu X, Xiao S, Chen B, Zhang F, Yao S, Wan Z, Yang D, Han H. Simultaneous determination of sildenafil, vardenafil and tadalafil as forbidden components in natural dietary supplements for male sexual potency by high-performance liquid chromatography-electrospray ionization mass spectrometry. J Chromatogr A. 2005; 1066(2):89-95.
4. M E Abdel Hamid. Determination of Sildenafil, Tadalafil, and Vardenafil in Tablets and Adulterated Herbal Products by ESI-MS-MS. Journal of Liquid Chromatography & Related Technologies. 2006; 29 (4): 591-603. doi: 10.1080/10826070500479393
5. Al Tahami Khaled. Determination of sildenafil, vardenafil and tadalafil in dietary supplements sold in the Yemeni market. International Journal of Scientific Research. 2014; 3: 403-405. doi:10.15373/22778179/apr2014/143.
6. Poposka Svirkova, Zaklina Shishovska, Maya Starkoska, K Arsova, Sarafinovska Zorica. Validated HPLC method for determination of sildenafil in pharmaceutical dosage forms. 2011; 21:25.
7. Venhuis BJ, de Kaste D. Towards a decade of detecting new analogues of sildenafil, tadalafil and vardenafil in food supplements: a history, analytical aspects and health risks. J Pharm Biomed Anal. 2012; 69: 196-208. doi: 10.1016/j.jpba.2012.02.014.

8. Saranjit Singh, Bhagwatprasad Akash, A Savaliyaravi, P Shah, Vikarantsinh M, Gohit Amandeepkaur. Strategies for characterizing sildenafil, verdenafil, Tadalafil and their analogues in herbal dietary supplements and detecting counterfeit products containing these drugs. Trends in Analytical chemistry. 2009; 28 (1):13-28.
9. Ulloa J, Sambrotta L, Redko F, Mazza ON, Garrido G, Becher EF and Muschietti L. Detection of a tadalafil analogue as an adulterant in a dietary supplement for erectile dysfunction. J Sex Med. 2015; 12:152–157.
10. Sibu C Padmanabhan. Overview on misuse of Sildenafil, Vardenafil, Tadalafil and its analogues in adulterated products in Malaysia. J Food Process Technol. 2015; 6:9 doi: 10.4172/2157-7110.s1.027
11. Man Che, Md Nor, Noorjuliana Lajis, Razak Lay, Harn Gam. Identification of sildenafil, tadalafil and vardenafil by gas chromatography mass spectrometry on short capillary column. Journal of chromatography A.2009; 1216:8426-8430. 10.1016/j.chroma.2009.10.016.
12. Sweetman, S C. Martindale-The Complete Drug Reference (33rd ed.). London, UK: Pharmaceutical Press. 2002.
13. Pawan Kumar Rai, Kinjal Modi. Orally disintegrating tablets: A novel approach for medication. International Journal of Medical and Health Research. 2019; 5 (1): 84-91.
14. Bojanapu A, Subramaniam AT, Munusamy J, Dhanapal K, Chennakesavalu J, Sellappan M, Jayaprakash V. Validation and method development of Tadalafil in bulk and tablet dosage form by RP-HPLC. Drug Res (Stuttg).2015; 65(2):82-85. doi: 10.1055/s-0034-1372608.
15. Coelho Neto J, Lisboa FLC. ATR FTIR characterization of generic brand-named and counterfeit sildenafil and Tadalafil based tablets found on the Brazilian market. Sci Justice. 2017; 57(4):283-295. doi: 10.1016/j.scijus.2017.04.009
16. Gad Haidy, El-Ahmady, Sherweit, Aboushoer, Mohamed, M Al-Azizi Mohamed. Application of Chemometrics in Authentication of Herbal Medicines: A Review. Phytochemical analysis. 2013; 24. doi:10.1002/pca.2378.
17. Ortiz RS, Mariotti KC, Schwab NV, Sabin GP, Rocha WF, de Castro EV, Limberger RP, Mayorga P, Bueno MI, Romão W. Fingerprinting of sildenafil citrate and tadalafil tablets in pharmaceutical formulations via X-ray fluorescence (XRF) spectrometry. J Pharm Biomed Anal. 2012; 58: 7-11
18. Coelho Neto J, Lisboa FLC. ATR FTIR characterization of generic brand-named and counterfeit sildenafil and Tadalafil based tablets found on the

Brazilian market. Sci Justice. 2017; 57(4):283-295. doi: 10.1016/j.scijus.2017.04.009

19. Hang Zhao, Wuliji Hasi, Lin Bao, Siqingaowa Han, Xuanyu Sha, Jia Sun, Xiutao Lou, Dianyang Lin, Zhiwei Lv. Rapid Detection of Sildenafil Drugs in Liquid Nutraceuticals Based on Surface-Enhanced Raman Spectroscopy Technology. Chinese Journal of Chemistry. 2017; 35(10):1522-1528.
20. Shin M, D Jee, R Chae, K Moffat Anthony. Identification of counterfeit Cialis, Levitra and Viagra tablets by near-infrared spectroscopy. Journal of Pharmacy and Pharmacology. 2005; 57:11.
21. Ganzera M, Choudhary MI, Khan IA. Quantitative HPLC analysis of withanolides in Withania somnifera. Fitoterapia.2003; 74 (2):68-76.
22. Deepak Mundkinajeddu,Laxman P Sawant, Rojison Koshy, Praneetha Akunuri,Vineet Kumar Singh,Anand Mayachari,Maged H, M Sharaf, Murali Balasubramanian, Amit Agarwal. Development and Validation of High Performance Liquid Chromatography Method for Simultaneous Estimation of Flavonoid Glycosides in Withania somnifera Aerial Parts. Analytical Chemistry. 2014; 351547: 1-3. http://dx.doi.org/10.1155/2014/351547,
23. S Rajasekar, R Elango. Estimation of alkaloid content of Ashwagandha (Withania somnifera) with HPLC methods. Journal of Experimental Sciences. 2011; 2(5): 39-41.
24. Abbas SS, Singh N. Anti-stress Agents (Herbs) of Indian Origin - Herbal Drugs, A twenty first century perspective. Delhi: Institute of Nuclear Medicine and Allied Sciences, Defence Research and Development Organization (DRDO), Govt. of India; 2006. pp. 578–591.
25. Matsuda Hisashi, Murakami Toshiyuki, Kishi Akinobu, Yoshikawa Masayuki. Structures of withanolides I, II, III, IV, V, VI, and VII, new withanolide glycosides, from the roots of Indian Withania somnifera and inhibitory activity for tachyphylaxis to clonidine in isolated guineapig ileum. Bioorganic & medicinal chemistry. 2011; 9: 1499-507. doi: 10.1016/S0968-0896(01)00024-4.
26. http://blogs.unimelb.edu.au/aurinands/files/2012/11/Using-Wards-Hierarchical-Clustering-Algorithm-to-Identify-Employment-Clusters-in-the-Northwest-Corridor-of-metropolitan-Melbourne.pdf. Accessed on: 8 Nov 2015.
27. The Unscramber manual. Camo Software AS http://www.camo.com.html. Accessed on: 8 Nov 2015
28. Gorry PA. General Least-Squares Smoothing and Differentiation by the Convolution (Savitzky-Golay) Method. Anal. Chem. 1990; 62: 570-3.
29. Luo J, Ying K, Bai J. Savitzky-Golay smoothing and differentiation filter for even number data. Signal Processing 2005; 85: 1429-34.

30. Neerak Kumar, Anita Yadav, Ranjan Gupta, Neeraj Aggrawal. Anti genotoxic effect of Withania somnifera (Ashwagandha) extract against DNA Damage induced by hydrogen peroxide in cultered human peripheral blood lymphocyte. Int.J.Curr.Microbial.App.Sci.2016;5(4):713-719. doi: 10 .20546/ijcmas.2016.504.082.